



HiFi Visual Target

Public Report



Author: **Stefan Nord**
Date: **2018-08-28**
Project within **Elektronik, Mjukvara och Kommunikation**

FFI Fordonsstrategisk
Forskning och
Innovation

VINNOVA

Energimyndigheten

TRAFIKVERKET

FKG

VOLVO

SCANIA

VOLVO

SCANIA

VOLVO

SCANIA

VOLVO

SCANIA

VOLVO

Contents

| | |
|--|-----------|
| 1 Summary | 4 |
| 2 Executive summary in Swedish | 4 |
| 3 Background | 5 |
| 4 Project Realization | 8 |
| 4.1 Organization and management..... | 8 |
| 4.2 Communication | 8 |
| 4.3 Work Packages and Execution | 9 |
| 4.4 Challenges and Experiences | 10 |
| 5 Objectives | 10 |
| 6 Results and deliverables | 11 |
| 6.1 Sensor Definition and Optical Characteristics..... | 11 |
| 6.2 Definition of targets | 14 |
| 6.3 Measurements on 3D Car Targets..... | 22 |
| 6.4 Measurements on Real Cars | 26 |
| 6.5 Measurements on 4a and DRi-2018 targets | 29 |
| 6.6 Measurements with Portable Optical Instrument | 32 |
| 6.7 Accelerated Ageing Tests and Measurements Setup..... | 35 |
| 6.8 Results from Optical Measurements..... | 45 |
| 6.9 Results from Geometrical Measurements..... | 62 |
| 6.10 Results Volvo Car Tests..... | 78 |
| 6.11 Results from Veoneer tests..... | 83 |
| 6.12 Delivery to FFI-goals | 87 |
| 6.13 Deliverables and Reports..... | 87 |
| 7 Dissemination and Publications | 88 |
| 7.1 Knowledge and Results Dissemination..... | 88 |
| 7.2 Publications | 88 |
| 8 Conclusions and Future Research | 89 |
| 8.1 Conclusions..... | 89 |
| 8.2 Future Research | 89 |
| 9 Participating Parties and Contact Persons | 90 |
| 10 References | 91 |

| | |
|--|-----------|
| Appendix A – Portable Optical Instrument..... | 92 |
| A1 Spectrometer..... | 93 |
| A2 Light source..... | 93 |
| A3 Reflection Probe..... | 93 |
| A4 Probe holder..... | 94 |
| A5 Integrating sphere..... | 95 |
| A6 Fibre cables..... | 95 |
| A7 Battery pack..... | 95 |
| A8 Software..... | 95 |

FFI in short

FFI is a partnership between the Swedish government and automotive industry for joint funding of research, innovation and development concentrating on Climate & Environment and Safety. FFI has R&D activities worth approx. €100 million per year, of which half is governmental funding. Currently there are five collaboration programs: Energy & Environment, Traffic Safety and Automated Vehicles, Electronics, Software and Communication, Sustainable Production Technology and Efficient and Connected Transport Systems. For more information:

www.vinnova.se/ffi

1 Summary

Advanced Driver Assistance Systems (ADAS) and Autonomous Driving (AD) vehicles rely heavily on sensors for achieving their goal of protecting the driver and passengers from potentially dangerous situations. Optical sensors are used to measure locations and velocities of objects at distances of up to 150 meters. Optical sensors could be cameras (for visible light or IR) used to detect either objects or road features (like e.g. road edges and markings). They are a common choice for high-end ADAS and are found in sensor sets of most AD vehicles.

To ensure reliable performance of object detection, extensive testing of optical sensors is required. In vehicle testing performed at test tracks like AstaZero, 3D soft car targets are used for safety reasons. However, due to non-perfect shape and materials, **the optical characteristics of 3D soft car targets may differ considerably from that of real vehicles** in traffic, resulting in different detection performance, and hence different activation of the functions. Moreover, during tests the quality of the 3D soft car targets deteriorates due to repeated impacts and reassembly of the targets, which implies that there is a **need of methods for securing the quality of the 3D soft car targets over time**.

By addressing these challenges, the goal of the project has been to contribute to improved testing methods of optical and geometrical characteristics of 3D soft car targets by:

- developing measurement methods and specifying measurement setups for the optical and geometrical characteristics of 3D soft car targets;
- developing simplified measurement methods for quality check on 3D soft car targets to secure the quality over time;
- providing input to international standardization regarding methods for measurement of optical and geometrical characteristics of real and soft car targets;

The project had a total budget of 4.9 MSEK and was coordinated by RISE Measurement Science and Technology. The list of participants is as follows:

- AstaZero AB
- RISE Measurement Science and Technology
- Veoneer
- Volvo Car Corporation (VCC)

The results include test of different measurement methods, different 3D soft car targets as well as real vehicles and also an accelerated ageing test of a 3D soft car target from DRi.

2 Executive summary in Swedish

Avancerade körstödssystem och autonoma fordon är starkt beroende av sensorer för att skydda förare och passagerare från farliga situationer. Optiska sensorer (typiskt kameror, LIDAR och laserscannern) används för att mäta position och hastighet på objekt på avstånd upp till 150 meter. För att säkerställa tillförlitligheten hos optiska sensorer behövs omfattande tester med mjuka s.k. surrogatmål. På grund av att form och material inte är idealt, kan de optiska egenskaperna hos surrogatmål skilja sig avsevärt från de egenskaper verkliga fordon har, vilket resulterar i varierande detekteringsprestanda samt otillförlitlig aktivering. Under testerna försämras dessutom kvaliteten hos de mjuka surrogatmålen, vilket innebär att det också finns ett behov av metoder för att säkra kvaliteten hos de mjuka surrogatmålen över tid. Projektet har utvecklat metoder och utfört mätningar på riktiga bilar såväl som mjuka bil-mål.

3 Background

There are three grand challenges the transportations of tomorrow face: environment, safety and congestion. One key element in meeting these challenges, and to reach the VisionZero stated by the Swedish government in 1997, is development of active safety systems and AD systems assisting or replacing the driver in both normal traffic situations as well as critical situations. These systems have already proven to decrease the number and severity of injuries and insurance cost [1]-[2]. The development of higher degree of AD puts stronger requirements on reliability, and therefore on its sensory input and the interpretation of this input. There exist several sensor types that typically are employed in sensor systems in ADAS and AD, such as visible spectrum and infrared cameras, laser scanners, ultrasonic sensors, and radars. In this project we focus on the optical sensors.

Camera sensors are an increasingly important part of active safety systems. They sense lane markings, obstacles, traffic signs and traffic participants with similar methods like human beings by evaluating the content of 2D or 3D road images. CMOS and CCD are the two main sensing techniques used in active safety camera sensors. With one video sensor the image “depth” can be only estimated by stadia metric means. With stereo video cameras the distance can be directly extracted for each position of the image. Direct speed measurement is not possible, neither with mono nor with stereo concept. The camera image is usually processed by sophisticated vision algorithms to recognize the relevant objects in the Region of Interest (RoI). The detection and classification algorithms are trained on the visual appearance of real objects and therefore it's important that the visible characteristic of the defined test object matches the ones of the real object as good as possible (i.e. pedestrian shape, posture, movement, extremity articulation, etc.). The most basic requirement for cameras relates to the overall dimensions of a target, its posture and contrast to the environment. While some current algorithms only use contour or chamfer lines to detect targets on the road the more advanced video systems already use a-priori information like the expected movements of the legs (i.e. gait recognition) to increase the classification rate for pedestrians.

LIDAR (LIght Detection And Ranging) is a technique used for remote sensing and measures the distance to objects by emitting and receiving short laser pulses. LIDARs commonly use the time-of-flight (TOF) principle for distance measurement, where a laser pulse is emitted, and the elapsed time is measured until the reflected signal is received again. The time delay between emission and reception is directly related to the distance due to the proportionality between TOF and distance. LIDARs use laser or LED light sources with wavelength in the NIR range and have detection ranges up to 200 m. Compared to RADAR sensors the beam-width is much smaller and sharper, which provides a much higher angular resolution. The performance of LIDARs decreases in adverse weather conditions like rain or snow or when the sensor gets blocked by e.g. dirt. The LIDAR sensor detection performance mainly depends on the NIR-reflectivity of the test objects. The test target must therefore be equipped with adequate reflecting parts. However, too big reflectors could saturate the LIDAR receiver especially in close proximity situations with a possible malfunction. Therefore, it is important that the reflection characteristic of the test object matches that of a real object as well as possible. Target requirements relate to reflection properties and tautness of the surface of the respective coverings.

In the 100 AD vehicles that Volvo Cars will build within the DriveMe project, the following optical sensors are used:

- Combined radar and camera: The combined 76 GHz frequency-modulated continuous wave radar and camera placed in the windscreen is the same as that in the all-new XC90. This system reads traffic signs and the road's curvature and can detect objects on the road such as other road users
- 360° surround vision: Four cameras monitor objects near the vehicle. Two are under the outer rear-view mirrors, one is in the rear bumper and one is in the grille. Besides detecting objects at close range, these cameras monitor lane markings. The cameras

have a high dynamic range and can handle very quick changes in lighting conditions, e.g. when entering a tunnel.

- Multiple beam laser scanner: This sensor system is placed in the front of the vehicle, below the air intake. The scanner can identify objects in front of the car and ensures very high angular resolution. It can also distinguish between objects. The unique laser sensor has a range of 150 meters for vehicles and covers a 140° field of view.
- Trifocal camera: Placed behind the upper part of the windscreen are three cameras in one, providing a broad 140° view, a 45° view and a long-range, yet narrow, 34° view for improved depth perception and distant-object detection. The camera can spot suddenly appearing pedestrians and other unexpected road hazards.

Low-cost, compact silicon-based vision sensors operating in the visible and near IR (wavelengths < 1 μm) with adequate dynamic range and response time can capture scene images with sufficient spatial resolution for automotive applications. Since vision is the main sensing modality used by human drivers, visual images must contain sufficient information for virtually all ADAS applications. The main challenge for silicon-based vision sensors in meeting automotive ADAS requirements is the dynamic range of the sensor, defined as the ratio of full-scale incident flux from a bright object to the noise equivalent flux of the sensor from a dim object. Both intra-scene and inter-scene wide dynamic ranges are important, since the vision sensor must handle a large range of lighting conditions from night time to daytime and scenes where objects in both dark shadow and bright sunlight must be seen in the same image. An intra-scene dynamic range of 110–120 dB is desirable to prevent image bloom-out. Such a vision sensor integrated with computer vision algorithms can extract pertinent scene information under most day and night weather conditions. The implementation of vision algorithms requires high performance solid state imaging processors with high computational throughput.

However, there are still factors that limit the accuracy and reliability of optical sensor systems, among which the most critical ones are:

- Huge within-class variabilities (targets may vary in shape, size, and color)
- Different reflectivity of material
- Illumination changes due to complex outdoor environments
- Wavelengths outside the visual spectrum makes it difficult for a human to determine what the target looks like from the optical sensor point of view
- Deposition of dirt, ice, snow and water on sensors

Validation of the optical sensor systems and identification of possible performance issues caused by the above factors, require extensive testing of the systems, both during optical sensor system development, and during verification of ADAS and AD vehicles. Controllability and safety of testing dictates that most testing is performed at closed test tracks. Since it is not possible to test situations that may result in collision with real vehicles, pedestrians etc. as targets, surrogate objects are used. These are typically mock-up objects made of soft materials that can be repeatedly hit without damage to themselves or the test vehicle [3]. To make testing with surrogate targets valid, sensor response of the surrogate target must be consistent with the response of the corresponding real target.

While several studies have been conducted where sensor-responses of cars and humans have been measured [4]-[5], most of the work has either been concentrated on radar sensor responses (RCS properties) of cars and humans or the optical characteristics of human targets [6]. Lacking is more thorough work on the optical response of car targets. Most of the work has also been focused on the tail aspects of car targets, but analysis of tail aspects provides validation for rear-end scenarios only. The aspects that might emerge in more complex traffic scenarios, for example, intersection collision avoidance [7], or merging, overtaking and cut-in cases for AD vehicles, where the optical sensor responses on target vehicles may vary rapidly, are not covered, limiting the applicability of the studied surrogate target for testing of these situations.

Moreover, analyses of other types of surrogate targets available on the market, as well as studies of possible improvements of the latter, are lacking. This poses limitations for OEMs, optical sensor developers and test tracks who need reliable surrogate targets for increasing need for reliable and safe optical sensor testing.

To address these issues, this project will consider the following questions:

1. How can the optical and geometrical characteristics of surrogate targets be assessed and validated against the real targets' characteristics by measurements? This, in turn, leads to the following question: What are the optical and geometrical properties of real targets?
2. How can surrogate targets be improved so that their optical and geometrical properties would better agree with real targets' ones?

During test track testing, surrogate targets can be deformed by repeating collisions. While their appearance can be inspected visually, internal deformations may lead to optical and geometrical characteristics changing in an unpredictable way, making further testing unreliable. Validation methods developed in this project can be applied to validate the targets after collisions and to identify when the characteristics have deteriorated, and repair is needed, either after the tests or by periodical calibrations.

To address the first question, we will specify measurement setups and develop methods for optical and geometrical characteristics that will be applicable to both real and surrogate targets. By using these measurement methods, we will assess the characteristics of real targets. This will provide the requirements on the surrogate targets (what should their characteristics be) and the results will be used to define how the surrogate targets need to be improved to fully function as valid test object for optical sensor development. We will investigate different strategies to improve the surrogate targets, and if possible implement and validate the most suitable ones.

In this project, we will focus on car targets as these are the most common test object types covering most scenarios. However, developed methods and tools should be generic and readily applicable to also other target types, for example pedestrians, trucks, bikes/motorcycles and animals.

4 Project Realization

This section describes the organization and execution of the project.

4.1 Organization and management

The project organization was kept as efficient as possible, but still followed the current best practice for this type of research. Project management structure was composed of:

- Steering Committee
- Project Manager
- Work package leaders

The steering committee consisted of one representative from each project partner. This representative had full power to decide on behalf of their respective organizations in matters of project management. The responsibility of the steering committee was to comprehensively ensure that the project reached its goals on time and with the right quality.

The steering committee had representatives from all partners:

| | |
|-----------|--------------------|
| VCC: | Per Hesselund |
| Veoneer: | Christian Svensson |
| RISE: | Stefan Nord |
| AstaZero: | Peter Janevik |

The project manager had the daily responsibility to ensure that the project reached all parts of the progress the planning prescribed. He handled all reporting and contact with VINNOVA and reported to the steering committee, if needed.

Each work package leader was responsible for planning and implementation of the respective work packages and ensured that the associated deliverables were undergoing internal review. Work package leaders were responsible for ensuring that work packages followed schedules and quality goals and reported any deviation during the project to the project manager.

4.2 Communication

Weekly Skype meetings were held throughout the project on every Wednesday 09:00-09:45 from October 2016 to June 2018. During these meetings a Trello board was used to follow up activities within the project. In addition to this, several physical meetings have also been held:

| Date | Location | Description |
|------------|---------------------|--|
| 2016-10-06 | AstaZero | Project Kick-Off Meeting |
| 2016-12-12 | Veoneer, Linköping | Sensor Workshop |
| 2017-03-02 | RISE, Borås | Project meeting and visiting RISE lab facilities |
| 2017-05-02 | Volvo Cars, Mölndal | Project Meeting |
| 2018-06-20 | AstaZero | Final Seminar |

A TeamPlace was set up for storage of project artefacts and for sharing of data.

4.3 Work Packages and Execution

The five work packages carried out in the project are outlined in Table 1 below.

| Work Package | Duration (months) | Activities | Results/deliverables |
|---|-------------------|--|---|
| WP1 Project management and Dissemination | Project | Management of the work performed in the project. | Status reports, presentations |
| WP2 Definition of targets and measurement methods | 6 | Define targets and measure methods for reliable, repeatable outdoor measurements of optical and geometrical characteristics of surrogate targets as well as real targets. | Reports on sensor definition, definition of targets, measurement methods and tools, and measurement validation. |
| WP3 Measurement System Setup | 6 | Definition of measurement system and test setup for measurements of reference targets and real vehicles. | Reports on test setups |
| WP4 Measurements and analysis of target characteristics | 9 | To obtain characteristics for real and surrogate targets by measurements and to derive requirements for target characteristics and develop methods and measures for validation of soft target characteristics. | Reports on measurement results |
| WP5 Demonstration | 3 | To demonstrate improved verification with developed tools and methods. | Final seminar and Final Report. |

Table 1 HiFi Visual Target Work Packages

The work package structure and their internal relationship are outlined below:

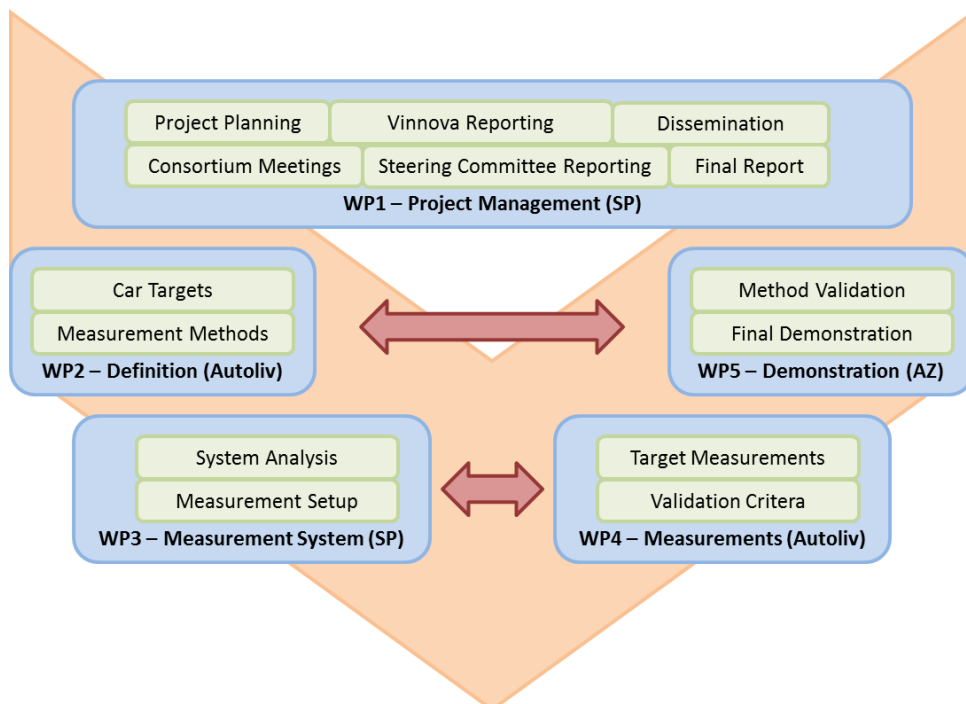


Figure 1 HiFi Visual Target work package structure and interdependencies

4.4 Challenges and Experiences

The main challenge within the project has been to have enough time and resource to analyse all the data from all measurements carried out within the project. We have done optical as well as geometrical measurements on 3 different 3D soft car targets as well as on 5 different real cars which in turn gave generated a large amount of data. The main focus has been to secure data by planning and coordinating all the measurement activities during in total 5 different occasions (4 occasions during 2017 and 1 occasion during 2018).

5 Objectives

The development of optical sensor system technology, a necessary sensing technology for active safety and AD vehicles, relies on reliable and efficient testing to validate the system performance. Efficient development requires early detection and solution of possible issues which the testing infrastructure must support.

The objective of the project as it was outlined in the application was to enable more efficient and reliable verification of optical sensor systems, including ADAS and AD systems that rely on the optical sensors, through:

- Development and validation of accurate and repeatable measurement methods of the optical and geometrical characteristics of visual car targets.
- Provide input to the development of more realistic surrogate car targets for safe testing of automotive optical sensor systems.
- Demonstration of improved verification with the developed measurement methods.
- Supporting international standardization (ISO) with standard methods enabling future verification and calibration of optical characteristics of active safety soft targets.

These goals have not changed during the project and has been reached. Having said that, we could of course have spent more time on analysing all the measurement data, but due to the large amount of data collected, there was not time enough within the project to run all the tests we could have done. We had to focus on the most important results to be able to make conclusions on the selected measurement methods. During the project, results have also been presented at the ISO committee meetings and there are ongoing discussions on how to incorporate the results from the project in to future updates of the standard.

6 Results and deliverables

6.1 Sensor Definition and Optical Characteristics

6.1.1 Situation Analysis

In ISO/WD 19206-3 [8] optical requirements for a Vehicle 3D Target (VT) are described. The draft standard includes the following optical sensor principles:

- CCD and CMOS camera sensors and stereo camera sensors
- Photonic Mixer Devices (PMD)
- Light Detection and Ranging (LIDAR)

Camera sensors cover the visible and NIR frequency spectra while PMD and LIDAR are more reliant on IR reflectivity of the target surface.

Other requirements are more generic and are mostly expressed in terms of visible vehicle features that the VT should resemble.

The 3D Vehicle Target Specification [9] from 4a (VT manufacturer) states that “the VT shall represent reflections of a real car, the windows (windscreen, side windows, rear window) shall look like transparent. They shall be illustrated by using a shining, polymer self-adhesive digital print film. For a more realistic representation, also the interior of a real car (seat, steering wheel, rear view mirror, driver) shall be indicated.”

The conclusion is that both standards and specifications currently are open for interpretations and there is a lack of scientific approach in determining what parameters are important for a VT to resemble a real target from an optical sensor perspective. As the VT are being used on test tracks it may change its properties with time due to collisions. This means that the standard should include tolerances that can be used for discarding a worn out VT and perhaps also to secure tolerances during production of VT:s.

In contrast to 3D car VT, more work has been done in studying VT for VRU:s (Vulnerable Road User). In [6] the IR reflectivity is specified in more detail with the IR reflectivity around 850 nm measured at both 45° and 90° at specified locations on the dummy.

There is certainly room for more work to improve existing requirements and measurement methods.

6.1.2 Definition of Sensors

To be able to define a suitable test setup and measurement methods we must define what type of optical sensors to focus on as well as determine what optical properties that will be important.

6.1.2.1 Camera Sensors

For the camera sensor the main importance of a target is that it resembles a true car as much as possible. To represent a reasonable range of cameras sensor variants the focus for this study should be in the visual spectrum.

6.1.2.2 LIDAR

For LIDAR sensors the reflectivity in the IR range up to 1000 nm should be covered.

6.1.3 Optical Signatures

Wavelengths of interest:

- 380 – 700 nm visual range for standard cameras
- Up to 1000 nm is possible with Si-based sensor
- ~905 nm infrared for laser range finder

Measuring instruments:

- Spectroradiometer
- Video photometer

Angular variation of sightline to target

6.1.4 Measuring Instruments

6.1.4.1 Spectroradiometer



- Spectrally resolved radiance/luminance from a surface defined by optics
- Spot measurement – no direct spatial information
- 2° to 0.125° measurement cone angle (2 – 35 mrad)
- Full spectral information 300 – 1100 nm allows matching to any sensor
- Lab instrument – not rainproof

6.1.4.2 Video Photometer



- Imaging, 5 MP
- Calibrated measure of luminance and color in the image
- May be spectrally matched to car sensor
- Cost ~500 kSEK

6.1.4.3 Visual/IR Spectroscopy

According to [9] the IR reflectivity shall be measured with a spectrometer e.g. Jaz – mobile miniature spectrometer from Ocean Optics, with wavelength range 350-1000 nm. Measurement probes with 45° and 90° shall be used.



According to [9] only 45° measurements were performed due to problems with stability of measurements at 90°. We decided to buy a similar instrument for measurements in the project.

6.1.4.4 Light Sources

- Solar (D65) lamp / CIE type A / LED headlamp
 - Different lamp types can be used
 - Spectrally characterized
- Laser illuminator
 - 800 – 900 nm
- Discrimination by gating and/or offset removal



6.2 Definition of targets

6.2.1 State of the art analysis

There are several vehicle target manufacturers creating equipment to validate and assess vehicle active safety sensors. Manufacturers include Messring, Anthony Best Dynamics (ABD), Dr. Steffan Datentechnik (DSD), Dynamic Research Inc. (DRI), Moshon Data and 4 Active Systems.

The target currently used (and since July 2013) for Euro NCAP (European New Car Assessment Programme) AEB City and Inter-Urban System testing is the Euro NCAP Vehicle Target (EVT) depicted in Figure 2. The EVT provides testing of AEB systems based on 24 and 77 GHz radar, LIDAR (Light Detection and Ranging), Camera and PMD (Photonic Mixing Device).



Figure 2 showing the EVT

The EVT consists of a balloon structure made of polyester, polyethylene, polyamide 6.6, polychloroprene and nylon. Inside the structure, at the rear of the target, there is a radar absorption mat constructed according to ASTM-D 1692-68 made of polyurethane foam. There is also a bumper element at the rear end which contains a radar reflector imitating a surface of 2.5 m² at 77 GHz. Finally, there are reflective films made of polyester mounted horizontally at the bumper and 600 mm above the bumper.

The outer cover of the EVT is made of PVC and has a car print which in turn has a retro-reflective film attached beneath the number plate. Looking at the target from the rear, between the wheels there is a radar absorption mat to mimic shadow underneath the mimicked vehicle. The EVT is 1600 mm wide, 1350 mm tall and 1000 mm deep. Suppliers of the EVT include Messring and Moshon Data [17].

6.2.2 3D Soft Car Targets

This section describes some of the existing 3D soft targets available on the market and which target planned to be used in Euro NCAP 2018 AEB.

6.2.2.1 Euro NCAP 2018 Global Vehicle Target (GVT)

The Euro NCAP 2018 AEB car-to-car test protocol uses a new global vehicle target shown below in Figure 3. It replicates a typical passenger vehicle in terms of visual, radar and LIDAR aspects [16].



Figure 3 The global vehicle target

6.2.2.2 DRi – Advanced test systems, Soft car 360

DRi Advanced Test Systems is a subsidiary of Dynamic Research Inc. and their focus is to develop and sell test devices and equipment for the automotive industry, located in California, USA. DRi has developed the Soft Car 360, of which the hatchback version is also the GVT to be used in Euro NCAP 2018. There are different versions of the target and the latest version offers:

- Realistic radar signature with radar reflective material in bumpers, doors and bonnet
- Reflective printed vehicle lights and number plates
- Radar absorbing material underskirts
- Foam wheels with corner reflectors
- Attachable side mirrors

Source of latest version capabilities: [12]

The latest version is depicted below in Figure 4, note the side mirrors, wheels and windows appearance change compared to Figure 3.



Figure 4 Depicts the latest version of the DRI Softcar 360 target, note the side mirrors, “see through” windows and wheel change compared to Figure 3.

Some of the specifications differ from the Euro NCAP GVT specifications on the Euro NCAP website but according to DRI [15] and Anthony Best Dynamics [12] the latest version will be used as GVT in Euro NCAP. The Soft Car 360 is manufactured by Anthony Best Dynamics under licensing from Dynamic Research Inc. and by Dynamic Research Inc. The chassis of the target is built from multiple foam pieces covered in vinyl which are attached together by Velcro. The chassis is then covered by a sheet with a car print to mimic a real vehicle. Figure 5 shows the chassis before the vinyl sheet is attached.



Figure 5 shows the chassis before being covered by the car print sheet [15].

6.2.2.3 4A – 4activesystems

4activeSystems is a company located in Traboch, Austria. They develop and produce both test equipment and target dummies for ADAS testing. Their free-standing car target, 4activeC2, is a 3D target with radar and visual properties like that of a real car. It weighs 55 kg and may be crashed in to from all directions at speeds up to 65 km/h. It is built in a modular system with zippers and fasteners, allowing rebuilding after collision with test vehicle. The target has reflective panels in the front and the rear and it has reflective license plates. 4A also produce other targets (bicyclist, pedestrian and motorcycle) and target carriers for their targets, 4activeXB and 4activeFB are compatible with the 4activeC2 target [10].



Figure 6 shows the 4activeC2 3D car target [10].

6.2.2.4 Moshon Data

Moshon Data is a company producing equipment for automotive safety testing based in Oxfordshire, UK. They manufacture the EVT and a towing system, Flex-Moshon EVT Towing System, as well as 3D targets and they have started developing motorcycle and pedestrian targets. They have a 3D target which looks like the GVT it is made of multiple pieces and covered by a vehicle print [18].

6.2.3 Target Carriers

The target carriers are used to propel the targets during dynamic testing. There are several manufacturers and some of the common properties of the carriers are: low profiles, following a path or driving behavior according to GPS and they are ok to run over by passenger vehicles.

6.2.3.1 High Speed Platform (HSP) - Veoneer

The HSP is developed by Veoneer and is used for internal research testing. It is made of aluminium and has a height of 90 mm except for the battery compartment which measures 120 mm. The ramps have an inclination of 8.5 degrees and the outer edge of the ramps have a rounded edge. It uses GPS with RTK correction data to follow pre-programmed drive files. It is waterproof, it can handle the weight of a heavy truck and a passenger vehicle may run in over at up to 100 km/h while the HSP is standing still. The HSP typically use the Soft Car 360 target for testing. The radar characteristics and visual properties remain to be investigated.



Figure 7 HSP Target Carrier.



Figure 8 HSP with the Soft Car 360 mounted.

6.2.3.2 Ultra-Flat Overrunable robot (UFO) - DSD

DSD has two different target carriers, UFO-50 and UFO-75. The UFO-50 is 1800x1800 mm and weighs 162kg. The UFO-75 is 2300x1800mm and weighs 235kg. They are both 98 mm tall when suspension is compressed, and they are made of aluminium. The UFO-50 has an 11° ramp angle. Figure 9 and Figure 10 below depicts the design of the UFO-50 and UFO-75 [19].

UFO-50 Size

1800 x 1800 mm incl ramps
1090 x 1090 mm frame

Frame: 98mm max height
11deg ramp angle

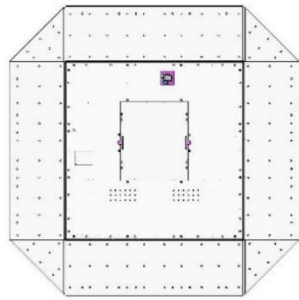


Figure 9 DSD – UFO-50 Size

UFO-75

No limitation in transportability
Max. transportation length retains

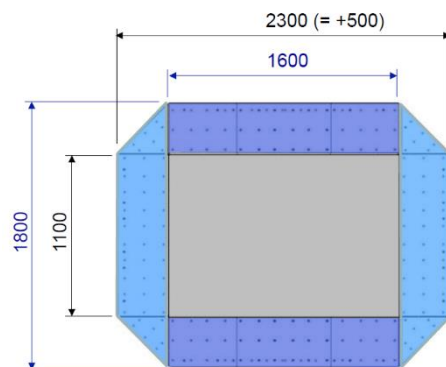
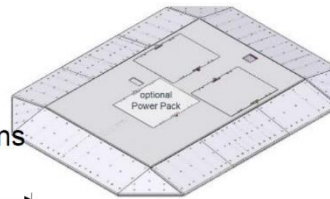


Figure 10 DSD – UFO-75 Size

6.2.3.3 Guided Soft Target vehicle (GST) – collaboration ABD & DRI

The Guided Soft Target Vehicle is developed by AB Dynamics and Dynamic Research Inc, ABD has developed the control system and DRI has developed the chassis. The GST can follow a pre-programmed path using GPS with correctional data. It is made of aluminium and weighs 315 kg. It is 2950 mm long, 1680 mm wide and 125 mm tall when suspension is compressed into the chassis [13].



Figure 11 Depicts the GST from ABD/DRI.

6.2.3.4 Heavy duty Guided soft target (GST HD) – collaboration ABD & DRI

The Heavy Duty Guided Soft Target Vehicle is developed by AB Dynamics and Dynamic Research Inc, ABD has developed the control system and DRI has developed the chassis, for testing heavy trucks. It is basically a more durable version of the original GST. The GST HD can, as the GST, follow a pre-programmed path using GPS with correctional data. It is also made of aluminium but weighs approximately 350 kg, this results in a maximum load of 9000 kg. It has the same length and width as the GST but it is 147 mm tall when suspension is compressed into the chassis [12].



Figure 12 shows the heavy-duty version of the GST from ABD/DRI.

6.2.3.5 4activefb – 4active systems

The 4activeFB is a free driving target carrier platform developed by 4activeSystems. It has a triangular shaped polymer cover and it is 50mm tall in general and 85mm tall at the three-wheel sections. It weighs 130 kg and is mostly used for vulnerable road user autonomous emergency brake (VRU AEB) system testing [11].



Figure 13 depicts the 4activeFB target carrier platform

6.2.4 Conclusions

There are numerous manufacturers of visual targets and target carriers for active safety testing. The information about the existing test products varies between different manufacturers. The common properties of the target carriers are that they are low, robust and GPS guided to follow preprogrammed paths to create different test scenarios for vehicle manufacturers and vehicle sensors manufacturers without introducing too much noise apart from what the actual 3D vehicle target creates. The main task of the target carriers is to invisibly propel the targets and, in case of a crash, not damage the test vehicle. In general terms the target carriers are quite equal and the thing that differentiates the different manufacturers are the user interface and the control systems. The conclusion is that HiFi Visual Target will use the target carriers available from project partners, one being the DSD UFO-75 the other being the HSP, for making the target characterization measurements.

Looking into the 3D targets, there are also numerous different models and versions. Some manufacturers have air-filled balloons and some manufacturers use foam blocks covered in reflective materials. The Euro NCAP only specifies one very specific target (or actually the properties of that target) to be used for AEB performance evaluation from 2018 and that is the SoftCar 360 developed by Dynamic Research Inc. Updates has been made since the document was published on Euro NCAP's website, and the latest version of the SoftCar 360 offers side mirrors and separate wheel parts amongst other things. The HiFi Visual target will use the SoftCar 360 as specified in the Euro NCAP specifications for measurements and analysis but also purchase the updated version to perform measurements to suggest improvements and compare to the old target.

6.3 Measurements on 3D Car Targets

6.3.1 Environment

The measurements took place in the Geometry facilities at RISE in Borås on February 27 – March 3 2017. For this purpose, the hall was prepared with covered windows so the light from our light source was dominant. In addition, the distances and angles to be used were marked by black tape on the floor, see Figure 14.

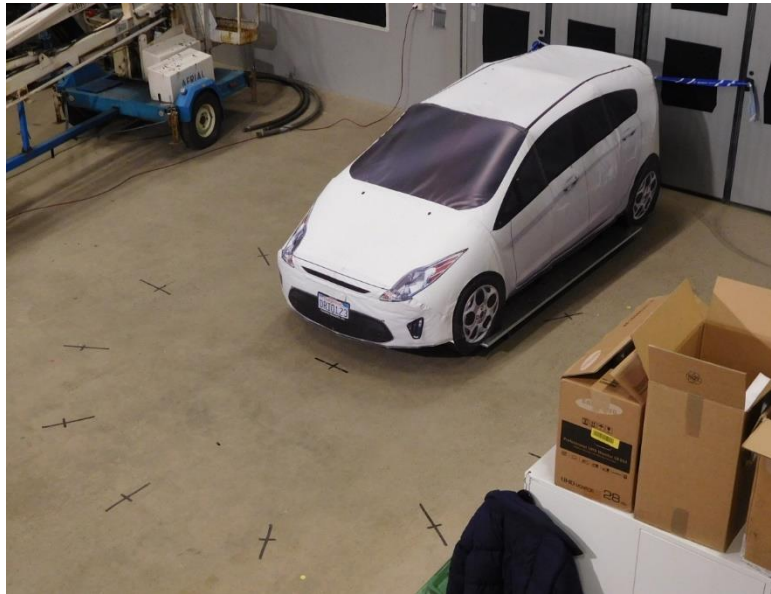


Figure 14. Soft car target 2 in the measurement hall.

A single light source was placed on a post, at 4,78 m above the ground and 7,30 m (horizontal distance) from the SCT measurement point, see Figure 15.



Figure 15. 1000-W halogen light source at 4,78 m height.

6.3.2 Measurement Objects

6.3.2.1 Soft Car Targets

Two Soft Car Targets were used in the measurements. Both were of the brand DRI (Dynamic Research, Inc., Torrance CA, USA). The model used was Soft Car 360® - Global Vehicle Target, which is based on a white 2009 model year Ford Fiesta car.

Soft car target 1 (SCT1) was supplied by AstaZero test track and had been used substantially in previous testing at AstaZero. It was visibly worn and had dark scuff marks on the sides. Figure 16 shows SCT1.



Figure 16. Soft car target 1 as used in measurements.

SCT2 was supplied by Veoneer AB and was the same model as SCT1 but had been used very little in testing. It had no visible marks. Figure 17 shows SCT2.

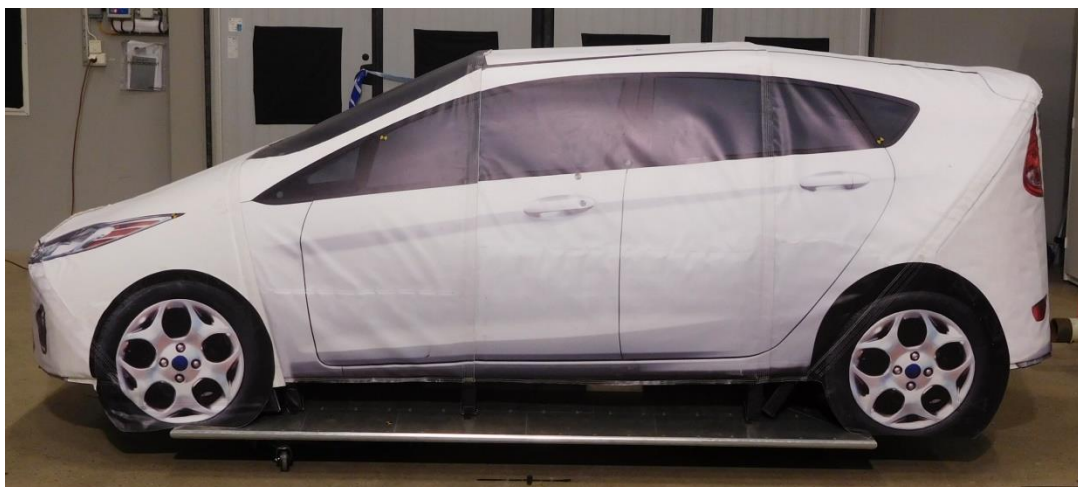


Figure 17. Soft car target 2 as used in measurements.

6.3.2.2 Target Carriers

SCT1 was equipped with a Target carrier from DSD. SCT 2 was supplied with a Target carrier made by Veoneer.

To handle the SCTs inside the measurement hall, they were each placed on four low dollies which enabled easy turning by hand. The wheels of the dollies are visible in Figure 16.

6.3.3 Equipment and Tools

6.3.3.1 Reflectance Measurement

Two different instruments were placed at a distance of 5,0 m from the SCT surface and used to record the reflected light from the target.

- Veoneer vehicle camera system
- Spectroradiometer (SR, Spectrascan PR-735)

As light source a 1000-W halogen lamp was placed in a position above and beyond the measurement instruments. In this way it emulates incident radiation from a low to medium height sun or oncoming vehicle headlights.

The Veoneer camera recorded video sequences of 30-s duration for each measurement direction. The SR was used to measure the reflected spectrum from different patches on the SCT surface. Each patch was of the approximate size 44 mm.

6.3.3.2 Geometry measurement

A terrestrial laser scanner (ZF 5010X) was used to capture the geometry of the car. The point cloud was also coloured in RGB using the scanners internal HDR camera.

6.3.4 Measurement Procedure

6.3.4.1 Reflectance Measurement

The reflectance was measured by the SR in ~100 patches distributed in the white areas around each SCT. The SCT was rotated in 30-degree steps the full revolution, enabling measurement from all horizontal aspects.



Figure 18. Spectroradiometer and Veoneer camera in the measurement position.

For each reflectance measurement, the spectral distribution of the light source can be considered and be adjusted to emulate solar, halogen, xenon, or LED lighting.

6.3.4.2 Geometry Measurement

The geometry measurements consist of two parts. The first part was carried out simultaneously as the reflectance measurement with the purpose of capturing the spatial data consistent with the reflectance data. The second part was carried out to check the impact of assembly.

6.3.4.2.1 Geometry measurement alongside reflectance measurement

The laser scanner was positioned alongside the reflectometer and at the same height, as close as practically possible (440 mm).

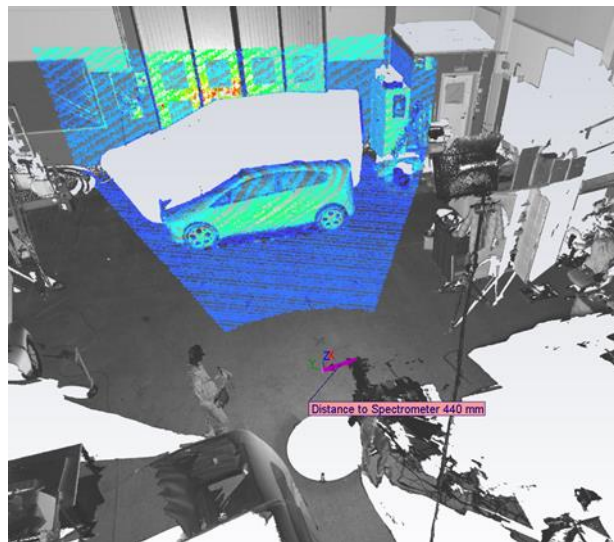


Figure 19 Positioning of laser scanner relative to reflectometer

The SCT's were then scanned in the same positions as for the reflectance measurements. The density of the point cloud on the surface of the SCT was approximately 2 mm.

6.3.4.2.2 Geometry measurement to check the impact of assembly

Each SCT was completely assembled 3 times. After each assembly the SCT was scanned covering the full geometry. The assembly were carried out by RISE personnel. For the Veoneer SCT, mounting supports manufactured by Veoneer personnel just prior to the tests were used. The SCT from AstaZero had no specific supports but were assembled directly on the carrier.



Figure 20 Result of one laser scan of SCT geometry

6.4 Measurements on Real Cars

The purpose of the measurement on real cars was to get reference data to be compared with measurements on the soft car targets (SCTs) to investigate differences in both geometrical shape and reflectance. This will provide valuable input on both the measurement method and how well the soft car targets resemble the optical and geometrical characteristics of real car targets.

6 different cars of different sizes, shapes and colour were selected (see Table 2). The project was also able to obtain a white Ford Fiesta MY 2011, which is the “raw model” for the soft 3D car target selected in ISO 19206-3. Most cars were “clean”, but for the Ford Fiesta, it was decided to do measurements both when it was relatively dirty and after it had been washed.

| Test slot: | 08:00-12:00 | | | 13:00-17:00 | | |
|------------|-------------|---------------------|-------------|-------------|---------------------|-------------|
| Date | Test object | Type and Properties | Supplied by | Test object | Type and Properties | Supplied by |
| 2017-06-12 | Ford Fiesta | White, "dirty" | RISE | MB E-class | White | Autoliv |
| 2017-06-13 | Volvo V40 | Magic Blue | VCC | Volvo XC 90 | Ember Black | VCC |
| 2017-06-14 | Volvo S90 | Luminous Sand | VCC | Volvo V90 | Silver Metallic | VCC |
| 2017-06-15 | Ford Fiesta | White, "dirty" | RISE | Ford Fiesta | White, "dirty" | RISE |
| 2017-06-16 | Ford Fiesta | White, "clean" | RISE | Ford Fiesta | White, "clean" | RISE |

Table 2 Test objects and test plan for the measurements during week 24 2017.

6.4.1 Environment

The measurements took place in the Geometry facilities at RISE in Borås on June 12 – June 16 2017. For this purpose, the hall was prepared with covered windows so the light from our light source was dominant. In addition, the distances and angles to be used were marked by black tape on the floor, see Figure 14.

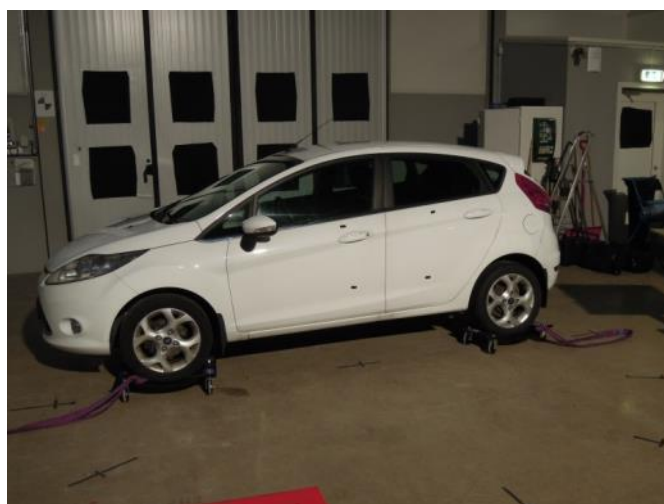


Figure 21. The white Ford Fiesta in the measurement hall.

A single light source was placed on a post, at 4,78 m above the ground and 7,30 m (horizontal distance) from the SCT measurement point, see Figure 15.

6.4.2 Measurement Objects

The measurement objects are shown in Figure 22 – Figure 26 . During the campaign it was decided to skip the silver metallic Volvo V90 due to that the time needed for the heavy Volvo XC90 was longer than expected (the wheel dolly could not support the weight, and the XC90 had to be moved by driving it).



Figure 22 White Ford Fiesta MY 2011



Figure 23 White Mercedes Benz E-Class



Figure 24 Magic blue Volvo V40



Figure 25 Ember black Volvo XC90



Figure 26 Luminous sand Volvo S90

6.4.3 Equipment and Tools

The same equipment and tools as described in chapter 6.3.3 was used.

6.4.4 Measurement Procedure

The same measurement procedures as described in chapter 6.3.4 were used.

6.5 Measurements on 4a and DRi-2018 targets

After measurements done on the old DRi-target (DRi Soft Car 360 Fiesta – Development Version) the project planned for similar measurements on both the new DRi-target (DRi Soft Car 360 Fiesta – Final Version 2018) and the 4activeC2 3D car target from 4activeSystems, in order to be able to compare with results from previous measurements.

6.5.1 Environment

The measurements took place in the Geometry facilities at RISE in Borås on October 6 – October 13 2017. The environment was the same as described in chapter 6.3.1.

6.5.2 Measurement Objects

6.5.2.1 4activeC2 3d car target

The 4activeC2 dummy is a free-standing 3D target with radar and visual properties, like a real car. The dummy is crashable up to 65 km/h from any direction and is rebuilt in two minutes by two people (not tested). For transport 4activeC2 can be disassembled. The car has reflective light, optionally available are active lights and indicators. For 4activeC2 spare parts include - label panels, locking system, wheels.



Figure 27. The 4activeC2 car target from 4activeSystems.

Key features according to manufacturer:

- easy to build up with a system of zippers and fasteners
- build up for first time in 10 min
- rebuild after a crash in 2 min - car stays in one shape after crash
- crashable up to 65 km/h without damages
- wheels are true dimensions - width and diameter
- modular system for transport and exchanging spare parts
- reflective light panels in the front and in the rear
- reflective license plate
- 3D side mirrors

6.5.2.2 DRi Soft Car 360 Fiesta – Final Version 2018

DRi has developed the Soft Car 360, of which the hatchback version is also the GVT to be used in Euro NCAP 2018. There are different versions of the target and according to the manufacturer the latest version offers:

- Realistic radar signature with radar reflective material in bumpers, doors and bonnet
- Reflective printed vehicle lights and number plates
- Radar absorbing material underskirts
- Foam wheels with corner reflectors
- Attachable side mirrors



Figure 28 The latest version of the DRI Soft Car 360 target, note the side mirrors, “see through” windows and more realistic wheels.

6.5.3 Equipment and Tools

The same equipment and tools as described in chapter 6.3.3 was used.

6.5.4 Measurement Procedure

The same measurement procedures as described in chapter 6.3.4 were used. In Figure 29 the 4activeC2 target is shown at the measurement facilities in Borås.



Figure 29 4activeC2 car target set up for measurements at RISE in Borås.

In Figure 30 the DRi Soft Car 360 target is shown at the measurement facilities in Borås.



Figure 30 DRi Soft Car 360 target set up for measurement at RISE in Borås.

6.6 Measurements with Portable Optical Instrument

Initial measurements with the portable optical instrument prototype was done on the DRi Soft Car 360 target. The purpose was to both get some feedback on the usability of the measurement equipment as well as investigating the time for assembling the target between collisions in preparations for the accelerated ageing tests planned for w10-13 2018. Geometrical scans were also performed at the beginning and end of the measurement activity.

6.6.1 Environment

The measurements were performed at Veoneer facilities in Vårgårda during w47-49 2017. Geometrical scans and the first tests of the optical reflectance measurement equipment were performed indoor. When colliding with the target and performing the assembly, the optical reflectance measurements were performed outdoor at *Carson city*, which is the Veoneer outdoor test facilities in Vårgårda.

6.6.2 Measurement Objects

For the initial tests both the old version and the final versions of the DRi Soft Car 360 target was used, but for collisions, only the old version of the DRI target was used.

6.6.3 Equipment and Tools

For the geometrical scans, the same equipment as described in chapter 6.3.3.2 was used. For the optical reflectance measurements, a portable equipment was developed, basically by putting the needed equipment in a box, so that measurements could be made outdoors regardless of weather conditions. The portable equipment is described in detail in Appendix A – Portable Optical Instrument.

6.6.4 Measurement Procedure

- Pieces of tape added to identify reference points to measure at. (Since there was no testing of ADAS functions at this time, the tape pieces should not make a difference).
- Changed naming of the data collected in the software for the measurement device to numbers to easily identify the data point with the physical point on the test target.
- During measurement kept a window open which showed the data files created during measurement, that way it was verified, during measurement, that no points were missed.

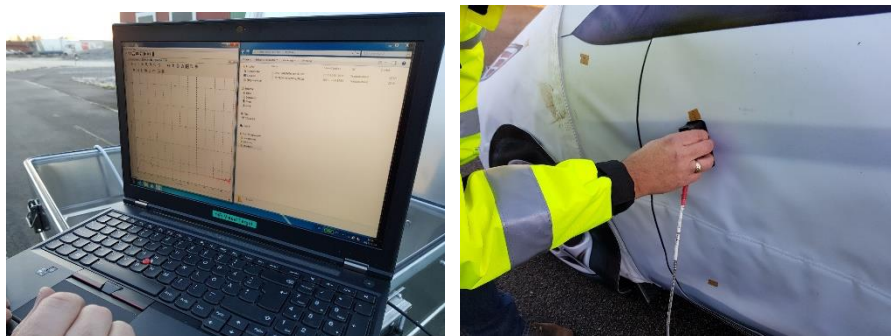


Figure 31 The portable optical reflectance measurement method. The picture to the left shows the laptop used for starting the measurement at each point. The picture to the right shows the probe at a specific measurement point on the target.



Figure 32 The target with measurement points indicated by pieces of tape.

| Name | Date modified | Type | Size |
|-----------------------------|------------------|---------------|-------|
| 20171204_Reflection_001.txt | 2017-12-04 13:26 | Text Document | 32 KB |
| 20171204_Reflection_002.txt | 2017-12-04 13:26 | Text Document | 32 KB |
| 20171204_Reflection_003.txt | 2017-12-04 13:26 | Text Document | 32 KB |
| 20171204_Reflection_004.txt | 2017-12-04 13:26 | Text Document | 32 KB |
| 20171204_Reflection_005.txt | 2017-12-04 13:26 | Text Document | 32 KB |
| 20171204_Reflection_006.txt | 2017-12-04 13:26 | Text Document | 32 KB |
| 20171204_Reflection_007.txt | 2017-12-04 13:26 | Text Document | 32 KB |
| 20171204_Reflection_008.txt | 2017-12-04 13:27 | Text Document | 32 KB |
| 20171204_Reflection_009.txt | 2017-12-04 13:27 | Text Document | 32 KB |
| 20171204_Reflection_010.txt | 2017-12-04 13:27 | Text Document | 32 KB |
| 20171204_Reflection_011.txt | 2017-12-04 13:27 | Text Document | 32 KB |
| 20171204_Reflection_012.txt | 2017-12-04 13:27 | Text Document | 32 KB |
| 20171204_Reflection_013.txt | 2017-12-04 13:27 | Text Document | 32 KB |
| 20171204_Reflection_014.txt | 2017-12-04 13:27 | Text Document | 32 KB |
| 20171204_Reflection_015.txt | 2017-12-04 13:27 | Text Document | 32 KB |
| 20171204_Reflection_016.txt | 2017-12-04 13:27 | Text Document | 32 KB |
| 20171204_Reflection_017.txt | 2017-12-04 13:27 | Text Document | 32 KB |
| 20171204_Reflection_018.txt | 2017-12-04 13:27 | Text Document | 32 KB |
| 20171204_Reflection_019.txt | 2017-12-04 13:27 | Text Document | 32 KB |
| 20171204_Reflection_020.txt | 2017-12-04 13:28 | Text Document | 32 KB |
| 20171204_Reflection_021.txt | 2017-12-04 13:28 | Text Document | 32 KB |
| 20171204_Reflection_022.txt | 2017-12-04 13:28 | Text Document | 32 KB |
| 20171204_Reflection_023.txt | 2017-12-04 13:28 | Text Document | 32 KB |
| 20171204_Reflection_024.txt | 2017-12-04 13:28 | Text Document | 32 KB |
| 20171204_Reflection_025.txt | 2017-12-04 13:29 | Text Document | 32 KB |
| 20171204_Reflection_026.txt | 2017-12-04 13:29 | Text Document | 32 KB |
| 20171204_Reflection_027.txt | 2017-12-04 13:30 | Text Document | 32 KB |
| 20171204_Reflection_028.txt | 2017-12-04 13:30 | Text Document | 32 KB |
| 20171204_Reflection_029.txt | 2017-12-04 13:30 | Text Document | 32 KB |
| 20171204_Reflection_030.txt | 2017-12-04 13:30 | Text Document | 32 KB |

Figure 33 Data files created during measurement

For the data handling, a Matlab script was written which converted the logged output (text files) into .mat files with data in order and ready to be processed using Matlab.

When colliding with the target and performing the measurements, the following workflow was used:

- Measure->
- crash ->
- build ->
-
- crash ->
- build ->
- Crash ->
- Build->
- Measure

The number of “crash+build” sequences before doing measurements will be dependent on how fast the target degenerates. When performing the reflectance measurements (referred to as “Measuring with Spectroscopy” in the column to the left in Figure 34), the time was measured. Also, the time for crashing and rebuilding (with 2 persons) the target was analysed (see the column to the right in Figure 34). In this way we could get an indication on how many collisions per day that will be possible.

- | | |
|---|---|
| <ul style="list-style-type: none"> ▪ Measuring with Spectroscopy (43points): <ul style="list-style-type: none"> - 9min 23s (calibration + “getting ready”) (split 5min 8s for measuring) - 4min 10s - Target moist(icy): 6min 12s - Conclusion: - Getting ready1 = 4min 15s - Getting ready2 = 4min 10s - Measure1=5min 8s - Measure2=6min 12s - Mean_Measure=5min 40s - Mean_Getting ready=4min 12s - Measuring should take 10min. | <ul style="list-style-type: none"> ▪ Building the target <ul style="list-style-type: none"> - 12min 15s (after 40km/h) 735 - 14min 25s (after 50km/h) 865 - 17min 54s (after 50km/h) 1074 - Mean= 14min 51s - But due to workload recommended building time=20min ▪ Crashing (incl. “reversing to start pos”): <ul style="list-style-type: none"> - 1st crash: 2min 4s - 2nd crash: 45s - 3rd crash: 1min 3s |
|---|---|

Figure 34 Timing for the optical measurements, crashing and building the target.

The conclusion based on these initial investigations was that maximum 20 collisions per day would be feasible.

6.7 Accelerated Ageing Tests and Measurements Setup

The purpose of the accelerated ageing tests and measurement was to get reference data to be compared with measurements done on the “mint condition” soft car targets to investigate differences in geometrical shape and reflectance after heavy use. This could provide valuable input on the measurement methods to be able to identify and define calibration criterions that could be used to decide if the target should be repaired or replaced.

6.7.1 Environment

The ageing tests and measurements took place at the City Area test track at AstaZero proving ground during w10 and w12 2018. The ageing tests were conducted as a series of collisions at 50 km/h speed hitting the soft car target in its rear part.



Figure 35 The Soft Car Target in the City Area of AstaZero proving ground.

6.7.2 Measurement Object

A Soft Car Target was used during the ageing tests and measurements. It was of the brand DRI (Dynamic Research, Inc., Torrance CA, USA) and the model used was Soft Car 360® - Global Vehicle Target, which is based on a white 2009 model year Ford Fiesta car. The soft car target was provided by Veoneer and was the same target used during previous measurements as a target in “mint condition”.



Figure 36 The Soft Car Target in “mint condition”

The soft car target was assembled on a plastic foam support that mimics the shape of a target carrier. In this way the soft car target will have the proper shape and at the same time minimized the risks related to collisions with a real target carrier.

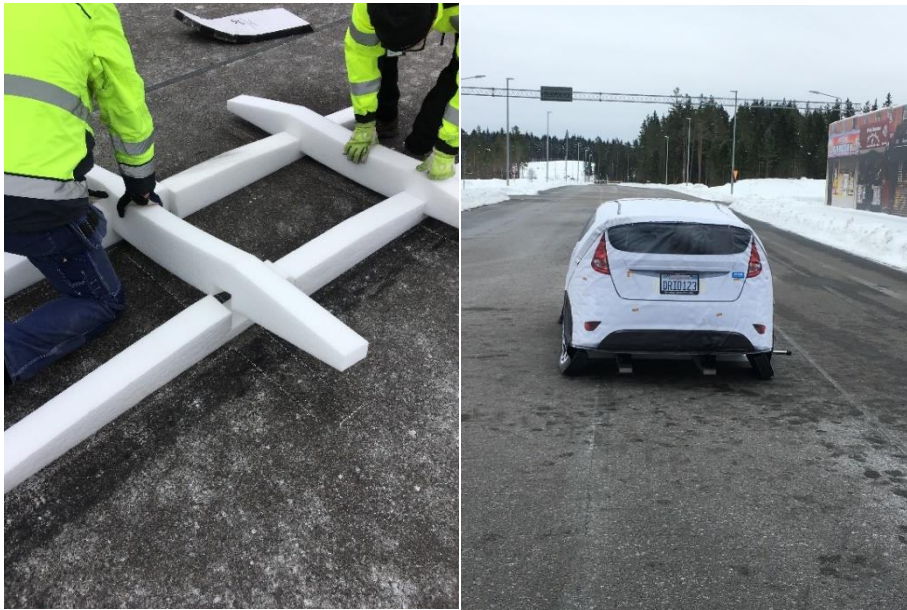


Figure 37 To the left: The plastic foam support used instead of a real target carrier. To the right: The soft car target assembled on the foam support and ready for collision

6.7.3 Equipment and Tools

6.7.3.1 Cars used for collisions

Two cars were used to collide with the soft car targets, one Mercedes from Veoneer and one Volvo V40 from AstaZero (see figures below). Both cars were prepared by adding impact protection as well as disabling of built in protection systems to prevent them to engage during the impact. Also, air bag systems had to be disabled for them not to be triggered accidentally.



Figure 38 The Mercedes from Veoneer, prepared with plastic coating in the front for impact protection and equipped with the Veoneer stereo camera system, in order to record raw data.



Figure 39 The Volvo V40 from AstaZero, covered with plastic sheet and foam in the front for impact protection.

6.7.3.2 Volvo Car Test Equipment

Volvo Cars used an XC90 equipped with both camera and radar systems and installed with logging equipment for data collection and analysis.

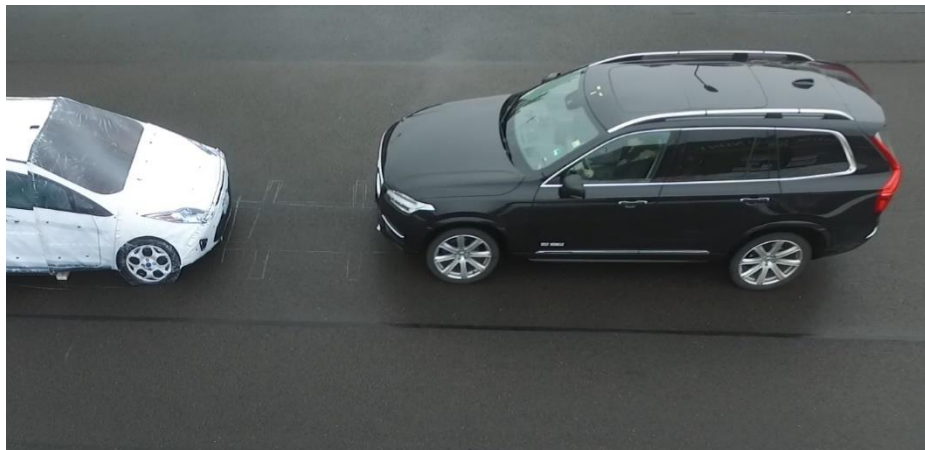


Figure 40 Volvo vehicle equipped with camera/radar system and logging equipment

6.7.3.3 Veoneer Car Test Equipment

Mercedes E-Class with a Veoneer stereo vision camera and a measurement system installed to collect the data.



Figure 41 The Veoneer vehicle equipped with stereo vision camera

6.7.3.4 Reflectance measurement

The portable reflectometry equipment described in D3.1 Optical Test Setup was used for reflectance measurements. The same measurements points indicated by tape was used.



Figure 42 The target with measurement points indicated with pieces of tape.

6.7.3.5 Geometry measurement

A terrestrial laser scanner (ZF 5010X) was used to capture the geometry of the car. The point cloud was also coloured in RGB using the scanners internal HDR camera.

In addition, a handheld scanner (Dotproduct DPI-8X) was tested to investigate its use in outdoor scanning of the soft car target in a proving ground environment.

6.7.3.6 Radar measurement

In cooperation with the HiFi Radar Target project, measurements of radar characteristics of the soft car target were also done to capture possible degradations of the target. The equipment is not described in this document. Below is a picture showing the radar scanning equipment used.



Figure 43 The radar scanning equipment from HiFi Radar Target project in action during the accelerated ageing tests and measurements.

6.7.4 Measurement Procedures

6.7.4.1 Collisions

The aim was to perform around 20 collisions per day at 50 km/h hitting the rear of the soft car target. The time needed for reassembly and setting up the soft car target for next collision varied between 6-15 minutes, depending on how many persons participated in the rebuild, weather conditions and, at the end the issue of getting the parts together due to that they started to wear down. For the 41 first hits, the Mercedes from Veoneer was used. For the rest of the hits, the Volvo V40 from AstaZero was used.



Figure 44 Pictures showing one of the 100 collisions, in this occasion with the Volvo V40

When getting close to 100 hits, the soft car target started to deteriorate to such a degree that the time and effort needed to assemble the target became too high. It was then decided to stop the procedure when reaching a total number of 100 hits.



Figure 45 Pictures showing the deterioration of the soft car target

6.7.4.2 Reflectance measurement

The reflectance was measured before any collision and then typically after 10 collisions.



Figure 46 The portable optical reflectance measurement equipment in action



Figure 47 Sampling the optical reflectance in two different points on the soft car target

6.7.4.3 Geometry measurement

The geometry was scanned with a laser scanner in the similar way as done in the indoor measurements done at RISE in Borås. The density of the point cloud on the surface of the SCT was approximately 2 mm. Geometry scans were done before any collisions, 3 times during the campaign, and finally, at the end, i.e. after 100 collisions. Along with the 3 laser scans during the campaign, the handheld scanner was also used.



Figure 48 Geometry scan of the soft car target in the City Area at AstaZero proving ground

6.7.4.4 Volvo Car Test procedures

Volvo Cars performed two sets of tests during the accelerated ageing tests at AstaZero. The first set was performed in the beginning of the accelerating ageing tests after very few collisions into the soft car target when it was still undamaged, and the second set of tests was performed after the 100 hits.

Two different test scenarios were performed during the two days.

1. The first was a CCRs (Car-to-Car Rear stationary), a scenario in which the vehicle travels forward towards a stationary vehicle and the frontal structure of the vehicle strikes the rear structure of the other in 0% overlap and in speeds 10 kph and 20 kph. This scenario is also part of the EuroNCAP protocol.
2. The second scenario was similar to the first with the difference that the frontal structure of the vehicle strikes the front structure of the other.

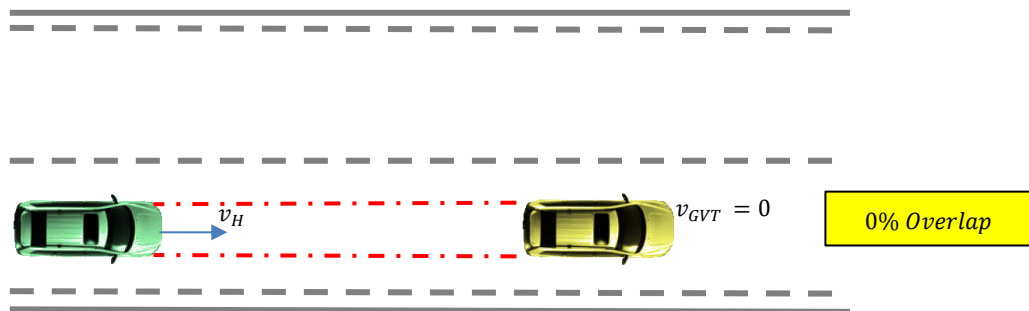


Figure 49 Rear collision scenario

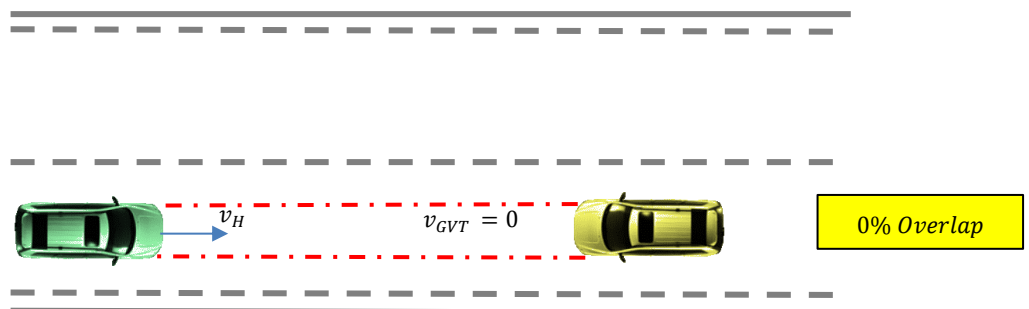


Figure 50 Front collision scenario

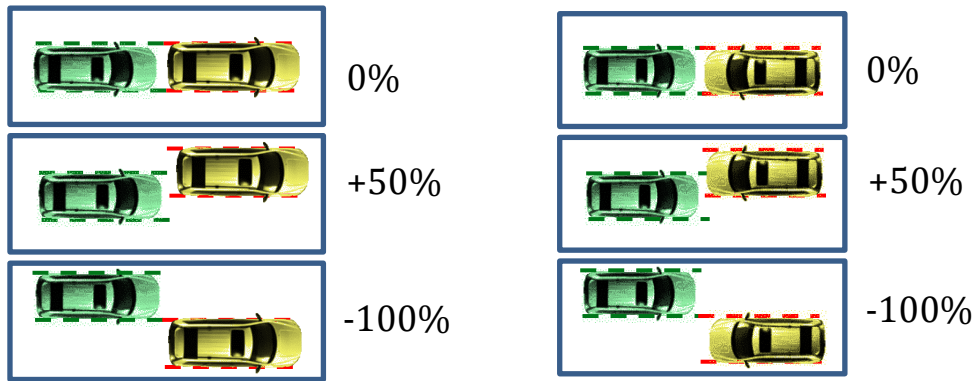


Figure 51 Overlap definition

Below the test cases during their execution at AstaZero proving ground are shown.



Figure 52 Rear collision scenario in the test track

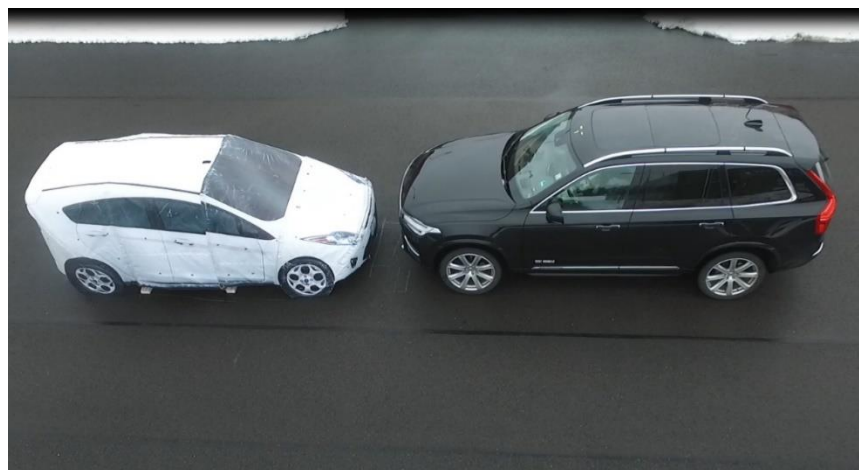


Figure 53 Front collision scenario in the test track

6.7.4.5 Veoneer Car Test procedures

The goal of the Veoneer test procedures was to record as many collisions with different impact points and different speeds to deliver as varying data as possible. The overall purpose is to

develop the camera's AEB (Autonomous Emergency Brake) function for the Euro NCAP test catalogue.

6.8 Results from Optical Measurements

The results from the optical measurements is based on the master thesis work done by two students at Luleå Technical University in cooperation with RISE. If more information about this thesis work is needed, please refer to "Characterization of visual and IR reflectivity for soft car targets" [20].

Figure 54 shows the visual changes that has happened to the 3D soft car target when hit repeatedly.



Figure 54 Before (top) and after (bottom) picture of the 3D soft car target

6.8.1 Reflectance Measurement Results

The 3D soft car target had 43 points marked on its shell to make sure all measurements were taken at the same spot on the target. These points were divided into four groups, left, right, front and back. The measurements contained data from 300-1150 nm and the areas from 400 to 800 nm and 890 to 920 nm were analysed.

These areas were chosen because 400 to 800 nm are the visible wavelengths for humans and 890 to 920 nm is part of the IR wavelengths.

In Figure 55, all 11 reflection measurements from the right side is shown. The first measurement had a mean reflectivity of 64 % and the last one had a mean value of 64.6 %.

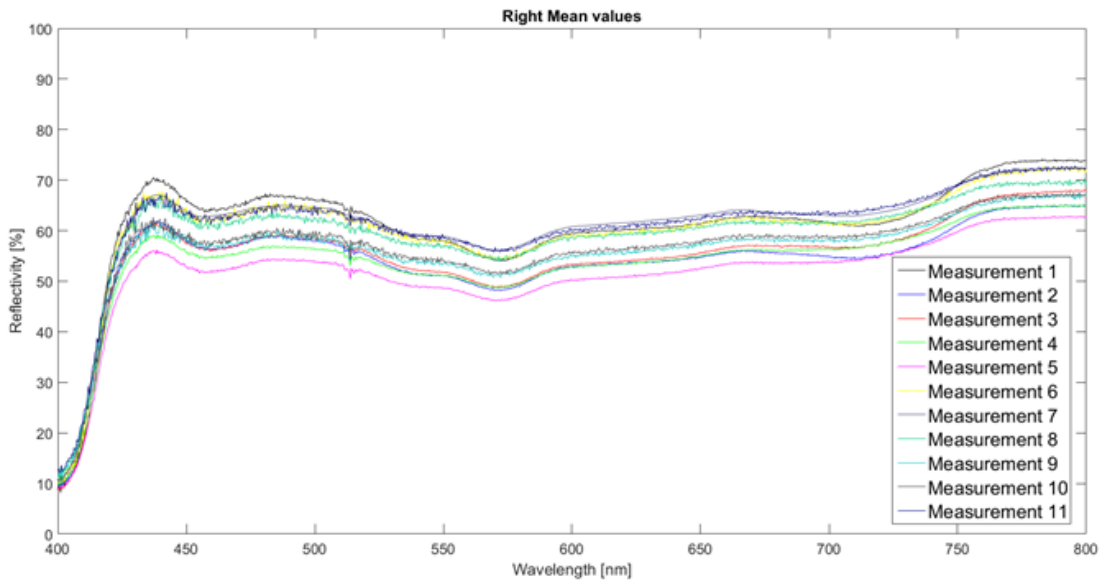


Figure 55 Right side

Figure 56 shows the reflection measurements from the left side. The first measurement had a mean reflectivity of 68.5 % and the last one had a mean value of 65 %.

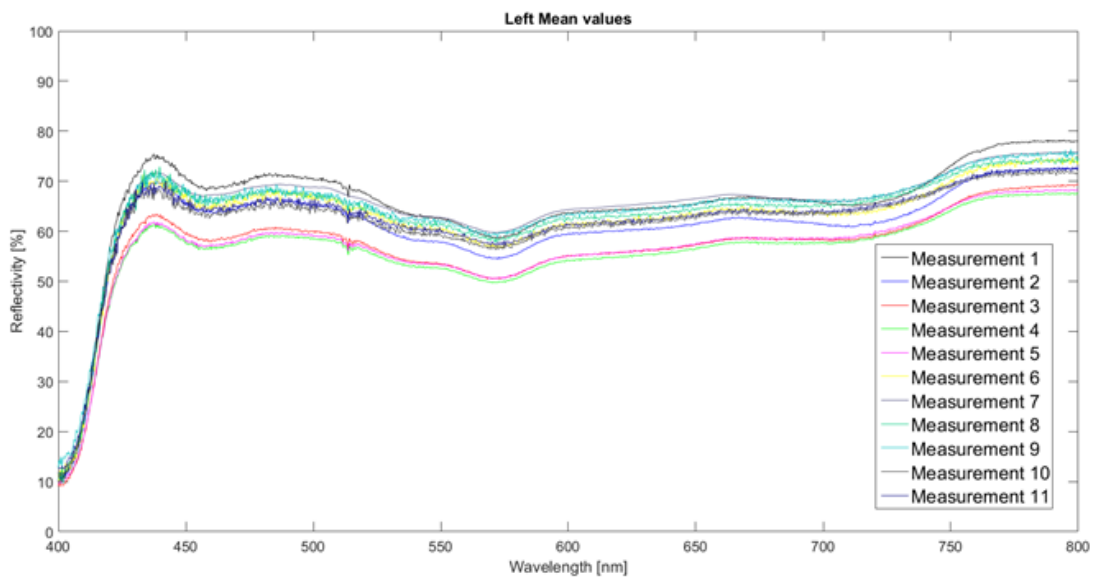


Figure 56 Left side

The reflection measurements from the front is shown in Figure 57. The first measurement had a mean reflectivity of 78.8 % and the last one had a mean value of 73.6 %.

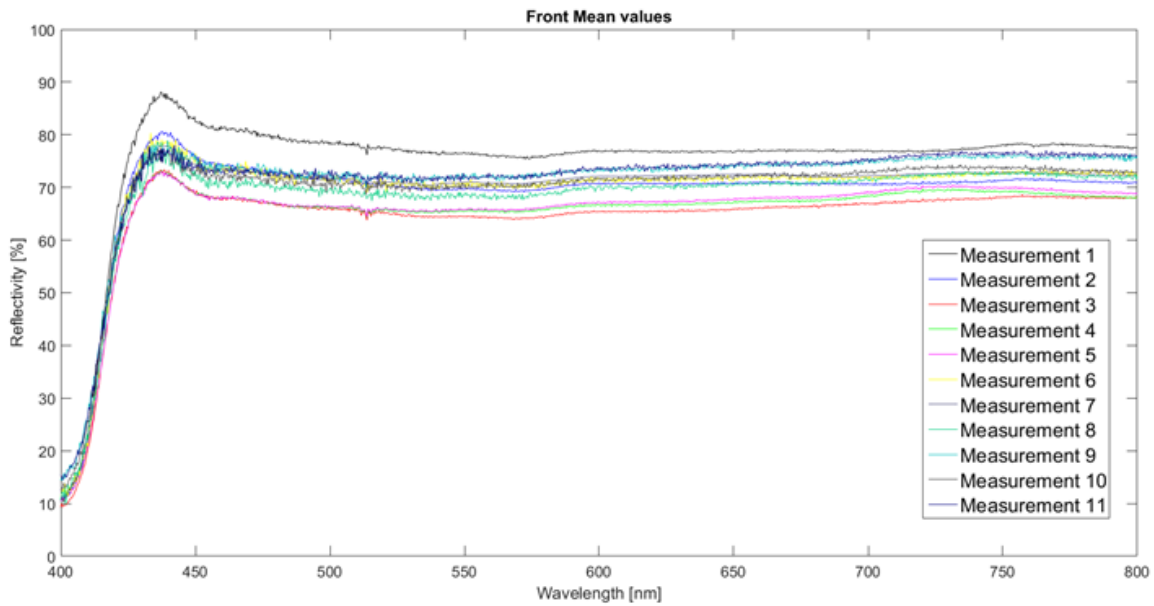


Figure 57 Front side

The rear-side measurements are shown in Figure 58. The first measurement had a mean reflectivity of 70.1 % and the last one had a mean value of 69.6 %.

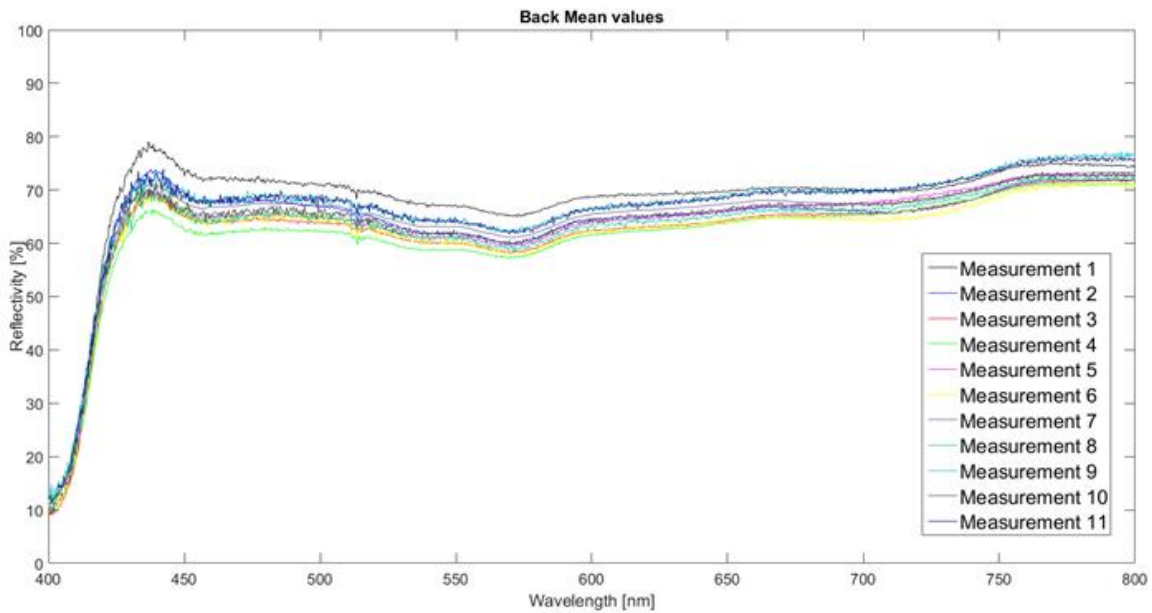


Figure 58 Rear side

Standard deviation and mean values for the different sides for all the reflection measurements are shown in Table 3.

| Left mean value | | | | | | | | | | | |
|--------------------|--------|--------|--------|-------|--------|-------|--------|-------|-------|-------|-------|
| Measurement | 1 | 2 | 3 | 4 | 5 | 6 | 7 | 8 | 9 | 10 | 11 |
| Mean Value | 68,5 | 63,65 | 59,75 | 59 | 59,25 | 65,5 | 67,625 | 67,25 | 67,45 | 64,5 | 65 |
| Standard Deviation | 8,22 | 9,69 | 8,60 | 12,85 | 11,18 | 8,59 | 9,94 | 7,86 | 12,31 | 10,07 | 10,58 |
| Right mean value | | | | | | | | | | | |
| Measurement | 1 | 2 | 3 | 4 | 5 | 6 | 7 | 8 | 9 | 10 | 11 |
| Mean Value | 64 | 56,675 | 56,8 | 56,6 | 54,625 | 63,35 | 63,85 | 63,2 | 58,85 | 59 | 64,6 |
| Standard Deviation | 7,49 | 9,59 | 7,48 | 8,88 | 8,01 | 8,07 | 9,65 | 9,92 | 12,14 | 10,79 | 7,63 |
| Front mean value | | | | | | | | | | | |
| Measurement | 1 | 2 | 3 | 4 | 5 | 6 | 7 | 8 | 9 | 10 | 11 |
| Mean Value | 78,825 | 71,975 | 66,545 | 67 | 67,25 | 71,75 | 71,8 | 69,95 | 73,35 | 72 | 73,61 |
| Standard Deviation | 4,83 | 7,26 | 12,16 | 9,64 | 7,90 | 10,96 | 6,86 | 6,62 | 7,53 | 7,46 | 6,79 |
| Back mean value | | | | | | | | | | | |
| Measurement | 1 | 2 | 3 | 4 | 5 | 6 | 7 | 8 | 9 | 10 | 11 |
| Mean Value | 70,15 | 65,95 | 65,125 | 64,9 | 66,145 | 64,45 | 67,08 | 65,79 | 69,66 | 65,98 | 69,6 |
| Standard Deviation | 9,68 | 10,15 | 14,23 | 8,65 | 8,88 | 12,74 | 11,53 | 10,33 | 9,69 | 12,61 | 8,54 |

Table 3 Standard deviation

In Figure 59, all 11 reflection measurements for the IR area on the right side are shown. The first measurement had a reflectivity of 70.8 % and the last one had a value of 70.6 %

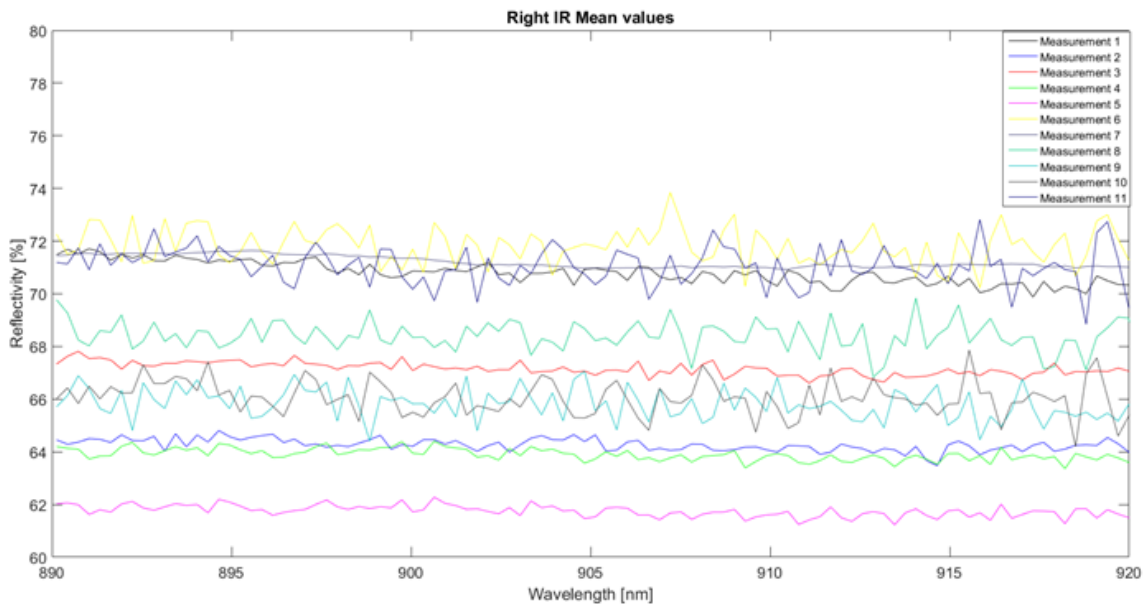


Figure 59 Right side IR

Figure 60 shows the reflection measurements for the IR area from the left side. The first measurement had a reflectivity of 75.4 % and the last one had a value of 70.9 %.

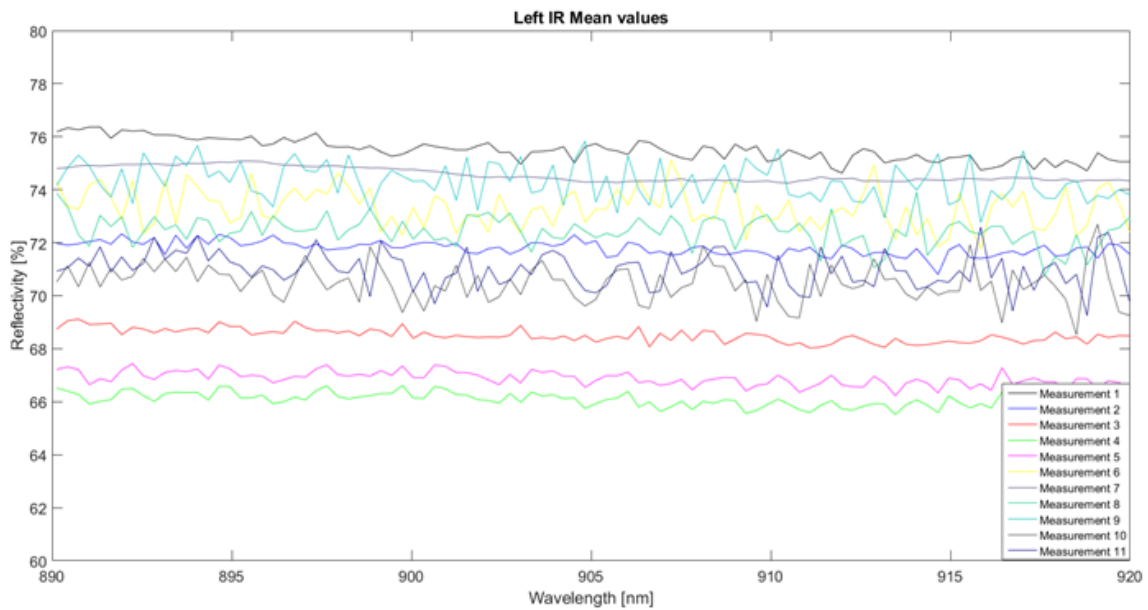


Figure 60 Left side IR

The reflection measurements for the IR area from the front are shown in Figure 61. The first measurement had a reflectivity of 74.4 % and the last one had a value of 74.1 %.

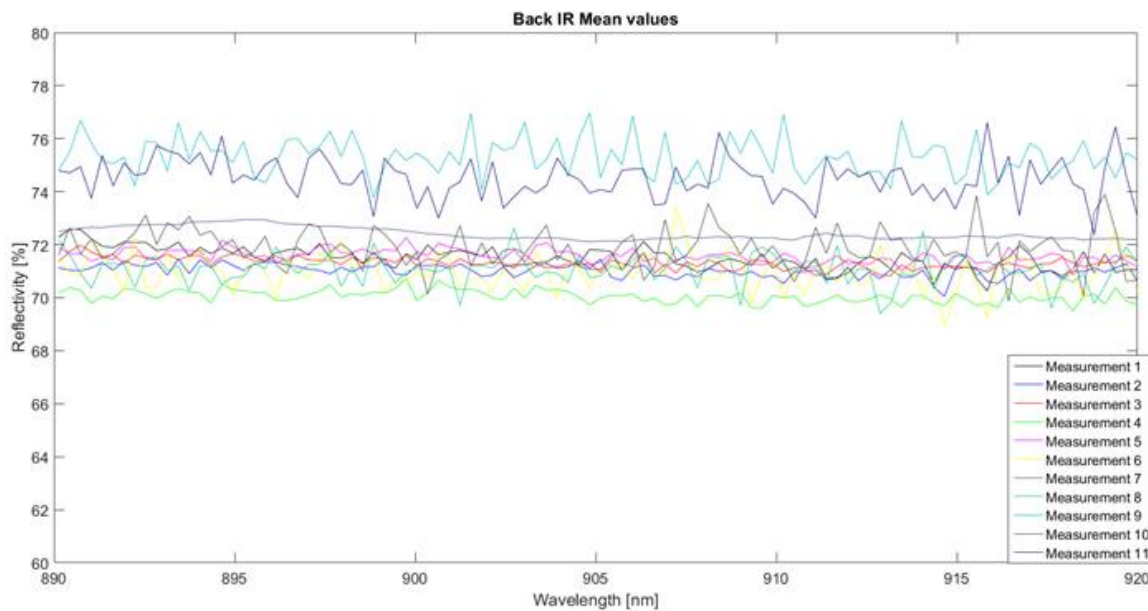


Figure 61 Front side IR

The rear-side measurements for the IR area are shown in Figure 62. The first measurement had a reflectivity of 71.4 % and the last one had a value of 74.5 %.

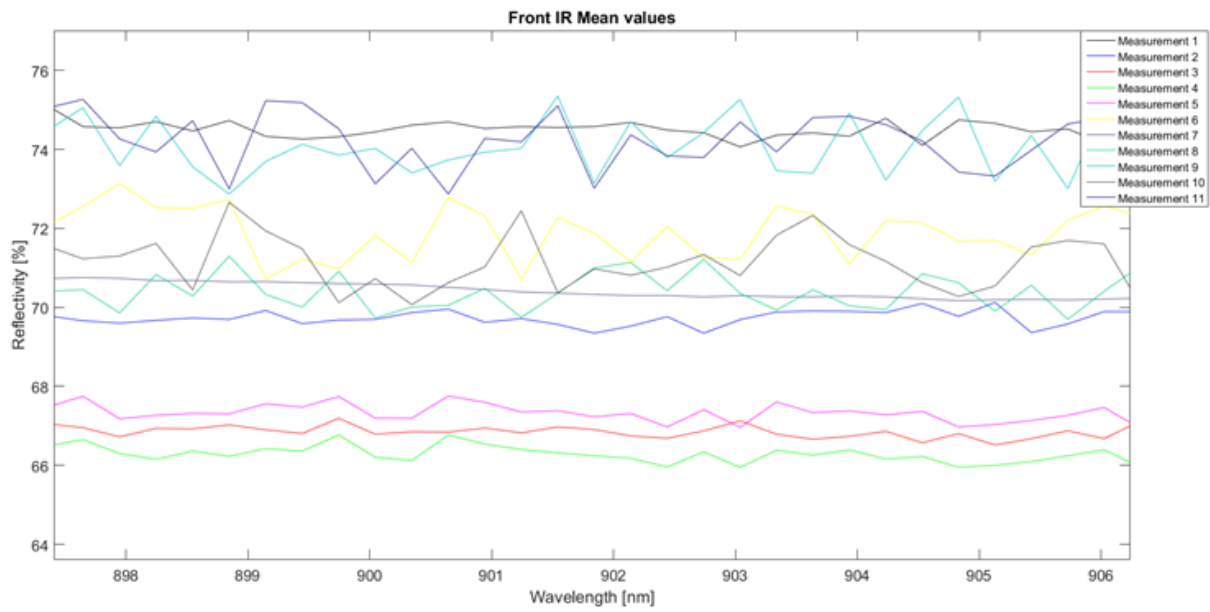


Figure 62 Rear side IR

6.8.2 RGB Response

Table 4 shows how the calculated RGB response for the different sides of the 3D soft car target changed between the measurements. These values are factors where 1 is the RGB response of a true white.

| RGB Response | | 1 | 2 | 3 | 4 | 5 | 6 | 7 | 8 | 9 | 10 | 11 |
|--------------|--|--------|--------|--------|--------|--------|--------|--------|--------|--------|--------|--------|
| Measurement | | | | | | | | | | | | |
| Right | | 0,6208 | 0,5492 | 0,5578 | 0,5474 | 0,5223 | 0,6127 | 0,6239 | 0,6040 | 0,5686 | 0,5752 | 0,6213 |
| Left | | 0,6641 | 0,6182 | 0,5744 | 0,5640 | 0,5717 | 0,6368 | 0,6611 | 0,6464 | 0,6541 | 0,6265 | 0,6328 |
| Front | | 0,7738 | 0,7090 | 0,6590 | 0,6680 | 0,6719 | 0,7149 | 0,7178 | 0,6994 | 0,7329 | 0,7150 | 0,7334 |
| Back | | 0,6963 | 0,6538 | 0,6346 | 0,6244 | 0,6479 | 0,6329 | 0,6616 | 0,6431 | 0,6775 | 0,6523 | 0,6759 |

Table 4 RGB response of the different sides

6.8.3 u'v' chromaticity results

In Figure 63 the result of u'v' for the rear side, and also x and y are shown. It also shows what colour each measurement has in Figure 64 and Figure 65.

| | x | y | u' | v' | CCT | Duv | Du'v' | Point symbol |
|----|--------|--------|--------|--------|------|---------|---------|--------------|
| 1 | 0,4654 | 0,4125 | 0.2652 | 0.5289 | 2639 | 0,0003 | 0,0004 | ● |
| 2 | 0,4660 | 0,4109 | 0.2663 | 0.5284 | 2619 | -0,0003 | -0,0005 | ● |
| 3 | 0,4676 | 0,4121 | 0.2668 | 0.5291 | 2607 | 0,0000 | 0,0000 | ● |
| 4 | 0,4694 | 0,4122 | 0.2679 | 0.5294 | 2585 | 0,0001 | -0,0001 | ● |
| 5 | 0,4686 | 0,4120 | 0.2675 | 0.5292 | 2593 | -0,0001 | -0,0002 | ● |
| 6 | 0,4668 | 0,4122 | 0.2663 | 0.5290 | 2617 | 0,0000 | 0,0001 | ● |
| 7 | 0,4678 | 0,4126 | 0.2667 | 0.5293 | 2608 | 0,0001 | 0,0002 | ● |
| 8 | 0,4679 | 0,4123 | 0.2669 | 0.5292 | 2605 | 0,0000 | 0,0000 | ● |
| 9 | 0,4680 | 0,4125 | 0.2669 | 0.5293 | 2605 | 0,0001 | 0,0001 | ● |
| 10 | 0,4681 | 0,4122 | 0.2671 | 0.5292 | 2601 | 0,0000 | 0,0000 | ● |
| 11 | 0,4676 | 0,4124 | 0.2667 | 0.5292 | 2609 | 0,0001 | 0,0001 | ● |

Figure 63 u'v' data for the rear side

Figure 64 shows the 1976 CIE $u'v'$ values for the rear side in a chromaticity diagram, and Figure 65 shows a zoomed picture of the same diagram.

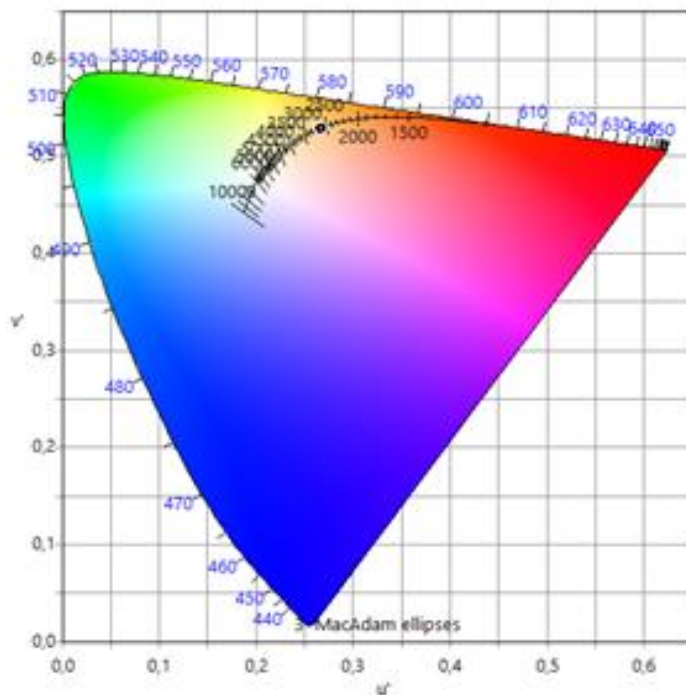


Figure 64 CIE 1976 $u'v'$ plot rear side

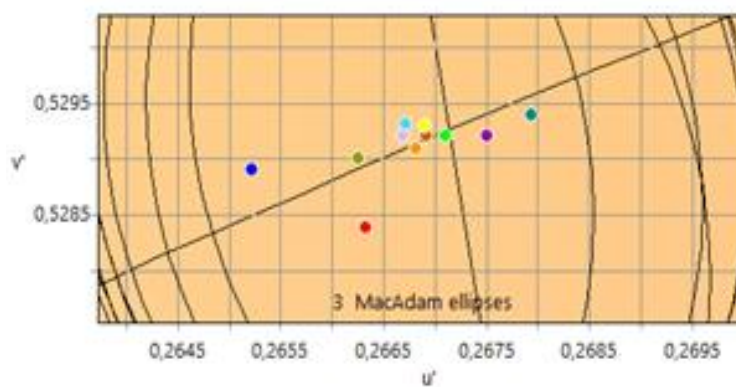


Figure 65 CIE 1976 $u'v'$ zoomed plot rear side

In Figure 66 the result of $u'v'$ for the front side, and x and y are shown. It also shows what colour each measurement has in Figure 67 and Figure 68.

| | x | y | u' | v' | CCT | Duv | Du'v' | Point symbol |
|----|--------|--------|--------|--------|------|--------|--------|--------------|
| 1 | 0,4645 | 0,4144 | 0.2638 | 0.5295 | 2665 | 0,0010 | 0,0015 | ● |
| 2 | 0,4651 | 0,4137 | 0.2645 | 0.5293 | 2652 | 0,0007 | 0,0010 | ● |
| 3 | 0,4659 | 0,4141 | 0.2648 | 0.5296 | 2645 | 0,0008 | 0,0012 | ● |
| 4 | 0,4672 | 0,4147 | 0.2654 | 0.5300 | 2631 | 0,0009 | 0,0014 | ● |
| 5 | 0,4678 | 0,4147 | 0.2658 | 0.5301 | 2623 | 0,0009 | 0,0013 | ● |
| 6 | 0,4665 | 0,4147 | 0.2649 | 0.5299 | 2642 | 0,0010 | 0,0015 | ● |
| 7 | 0,4672 | 0,4149 | 0.2653 | 0.5301 | 2633 | 0,0010 | 0,0015 | ● |
| 8 | 0,4677 | 0,4145 | 0.2658 | 0.5300 | 2624 | 0,0008 | 0,0012 | ● |
| 9 | 0,4681 | 0,4151 | 0.2658 | 0.5303 | 2623 | 0,0010 | 0,0015 | ● |
| 10 | 0,4679 | 0,4149 | 0.2657 | 0.5302 | 2625 | 0,0010 | 0,0014 | ● |
| 11 | 0,4689 | 0,4153 | 0.2662 | 0.5305 | 2614 | 0,0010 | 0,0015 | ● |

Figure 66 $u'v'$ data for the front side

Figure 67 shows the 1976 CIE $u'v'$ values for the front side in a chromaticity diagram, and Figure 68 shows a zoomed picture of the same diagram.

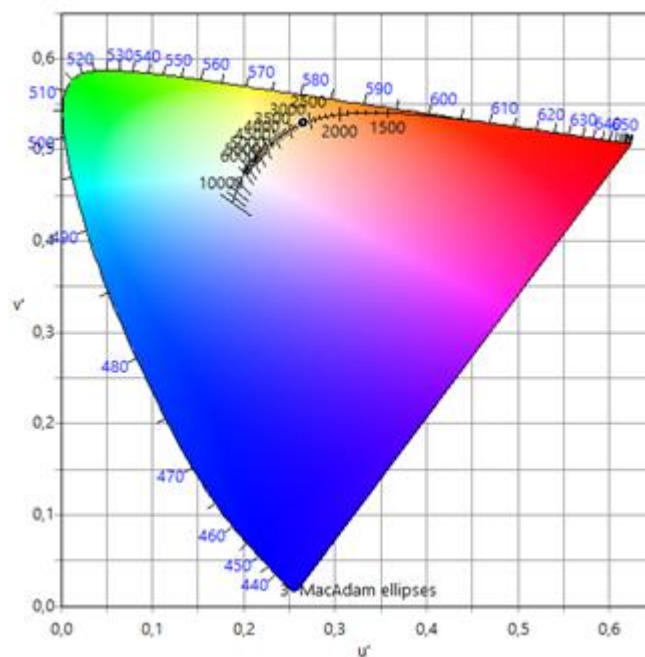


Figure 67 CIE 1976 $u'v'$ plot front side

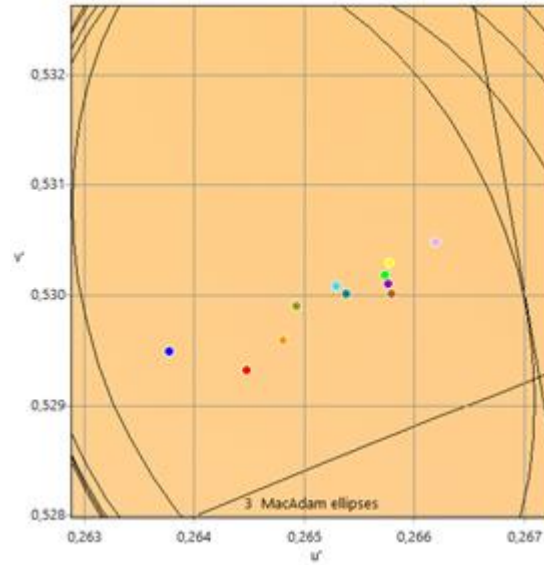


Figure 68 CIE 1976 $u'v'$ zoomed plot front side

In Figure 69, the results of $u'v'$ for the right side, and x and y are shown. It also shows what colour each measurement has in Figure 70 and Figure 71.

| | x | y | u' | v' | CCT | D_{uv} | $D_{u'v'}$ | Point symbol |
|----|--------|--------|--------|--------|------|----------|------------|--------------|
| 1 | 0,4623 | 0,4108 | 0.2640 | 0.5278 | 2667 | -0,0001 | -0,0002 | ● |
| 2 | 0,4637 | 0,4105 | 0.2650 | 0.5279 | 2647 | -0,0003 | -0,0005 | ● |
| 3 | 0,4640 | 0,4112 | 0.2649 | 0.5282 | 2648 | -0,0001 | -0,0002 | ● |
| 4 | 0,4658 | 0,4118 | 0.2658 | 0.5287 | 2628 | 0,0000 | 0,0000 | ● |
| 5 | 0,4660 | 0,4120 | 0.2658 | 0.5288 | 2628 | 0,0000 | 0,0001 | ● |
| 6 | 0,4639 | 0,4120 | 0.2645 | 0.5285 | 2655 | 0,0002 | 0,0003 | ● |
| 7 | 0,4661 | 0,4122 | 0.2658 | 0.5289 | 2627 | 0,0001 | 0,0002 | ● |
| 8 | 0,4656 | 0,4119 | 0.2656 | 0.5287 | 2632 | 0,0000 | 0,0000 | ● |
| 9 | 0,4661 | 0,4125 | 0.2657 | 0.5290 | 2629 | 0,0002 | 0,0003 | ● |
| 10 | 0,4659 | 0,4123 | 0.2656 | 0.5289 | 2631 | 0,0002 | 0,0002 | ● |
| 11 | 0,4658 | 0,4126 | 0.2654 | 0.5290 | 2635 | 0,0003 | 0,0004 | ● |

Figure 69 $u'v'$ data for the right side

Figure 70 shows the 1976 CIE $u'v'$ values for the right side in a chromaticity diagram, and Figure 71 shows a zoomed picture of the same diagram.

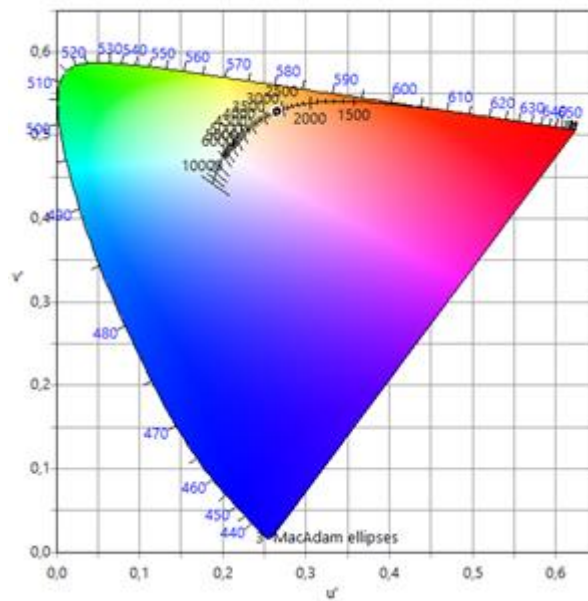


Figure 70 CIE 1976 $u'v'$ plot right side

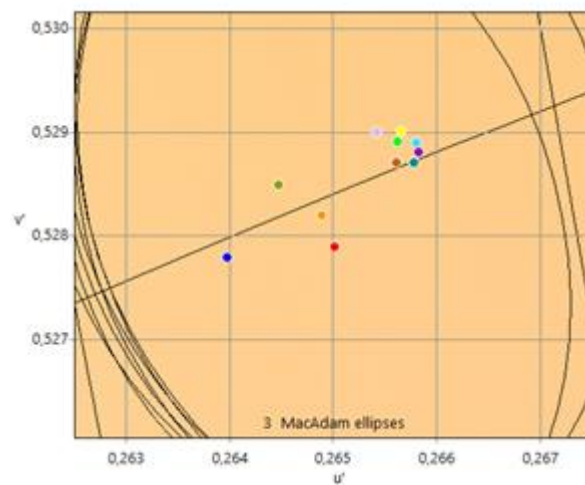


Figure 71 CIE 1976 $u'v'$ zoomed plot right side

In Figure 72 the result of $u'v'$ for the left side, and x and y are shown. It also shows what colour each measurement has in Figure 73 and Figure 74.

| | x | y | u' | v' | CCT | D_{uv} | $Du'v'$ | Point symbol |
|----|--------|--------|--------|--------|------|----------|---------|--------------|
| 1 | 0,4620 | 0,4115 | 0.2635 | 0.5280 | 2677 | 0,0001 | 0,0002 | ● |
| 2 | 0,4630 | 0,4108 | 0.2644 | 0.5279 | 2659 | -0,0002 | -0,0002 | ● |
| 3 | 0,4643 | 0,4114 | 0.2650 | 0.5283 | 2645 | 0,0001 | 0,0001 | ● |
| 4 | 0,4650 | 0,4116 | 0.2654 | 0.5285 | 2637 | 0,0000 | 0,0001 | ● |
| 5 | 0,4657 | 0,4118 | 0.2657 | 0.5287 | 2630 | 0,0000 | 0,0000 | ● |
| 6 | 0,4636 | 0,4122 | 0.2642 | 0.5285 | 2661 | 0,0003 | 0,0004 | ● |
| 7 | 0,4651 | 0,4123 | 0.2651 | 0.5288 | 2642 | 0,0002 | 0,0003 | ● |
| 8 | 0,4641 | 0,4122 | 0.2645 | 0.5286 | 2654 | 0,0003 | 0,0004 | ● |
| 9 | 0,4649 | 0,4124 | 0.2649 | 0.5288 | 2646 | 0,0003 | 0,0004 | ● |
| 10 | 0,4652 | 0,4123 | 0.2652 | 0.5288 | 2640 | 0,0002 | 0,0003 | ● |
| 11 | 0,4647 | 0,4125 | 0.2648 | 0.5288 | 2648 | 0,0003 | 0,0005 | ● |

Figure 72 $u'v'$ data for the left side

Figure 73 shows the 1976 CIE $u'v'$ values for the left side in a chromaticity diagram, and Figure 74 shows a zoomed picture of the same diagram.

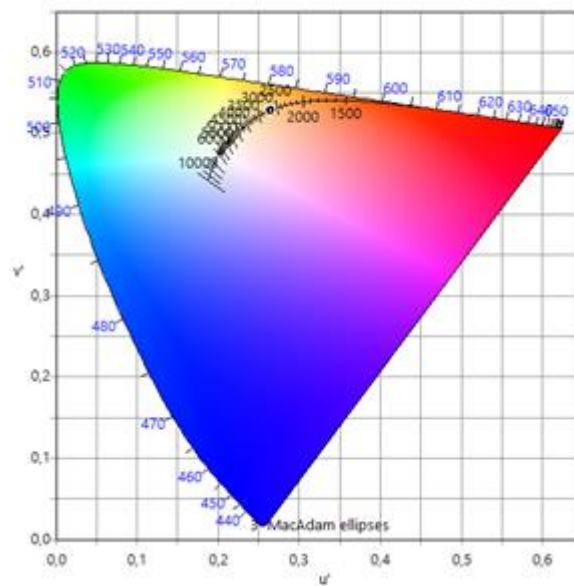


Figure 73 CIE 1976 $u'v'$ plot left side

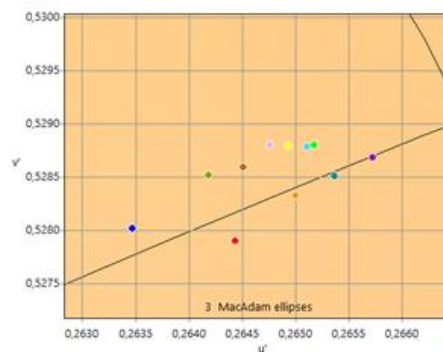


Figure 74 CIE 1976 $u'v'$ zoomed plot left side

6.8.4 Comparison between portable measurement equipment and PR-735

A comparison was made between the PR-735 spectroradiometer and the portable measurement equipment. The object measured was a Ford Fiesta 2011 that was newly washed. Figure 75 and Figure 76 show the spectral reflectance graphs.

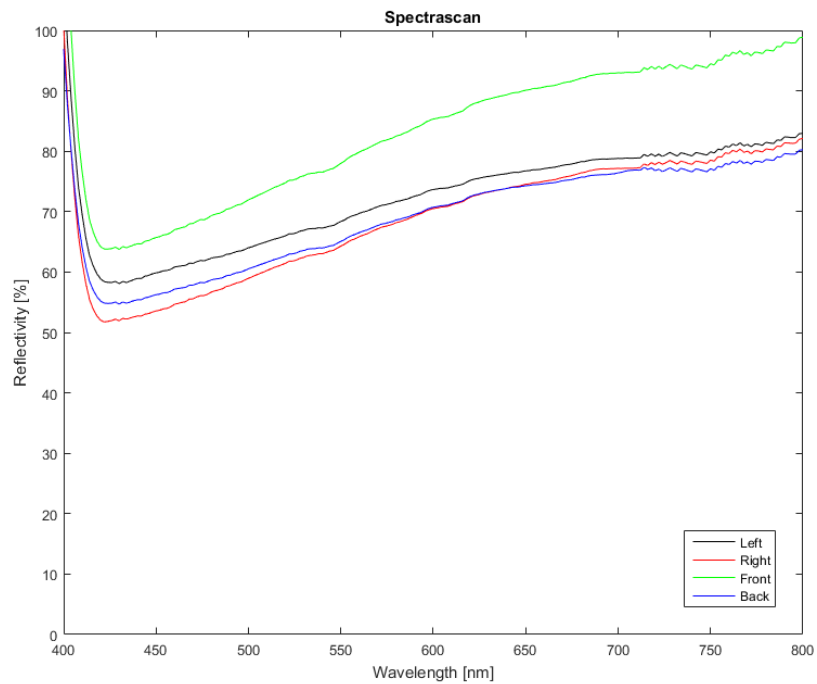


Figure 75 Spectral reflectivity with the spectroradiometer

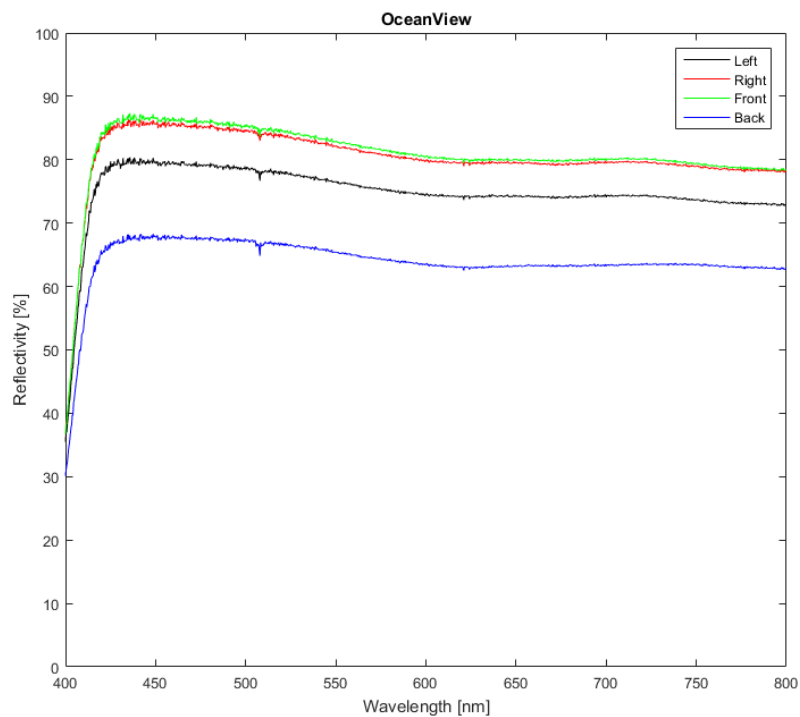


Figure 76 Spectral reflectivity with the portable measurement equipment

Figure 77 shows the calculated $u'v'$ values for the spectroradiometer measurements. Figure 78 shows the chromaticity diagram and Figure 79 show a more zoomed in version of the same diagram.

| | x | y | u' | v' | CCT | Duv | Du'v' | Point symbol |
|---|--------|--------|--------|--------|------|--------|--------|--------------|
| 1 | 0,4342 | 0,4093 | 0,2466 | 0,5230 | 3089 | 0,0025 | 0,0035 | ● |
| 2 | 0,4290 | 0,4074 | 0,2441 | 0,5215 | 3164 | 0,0025 | 0,0036 | ● |
| 3 | 0,4298 | 0,4078 | 0,2444 | 0,5218 | 3154 | 0,0026 | 0,0037 | ● |
| 4 | 0,4319 | 0,4089 | 0,2453 | 0,5225 | 3126 | 0,0027 | 0,0038 | ● |

Figure 77 $u'v'$ data from the Spectrascan measurement

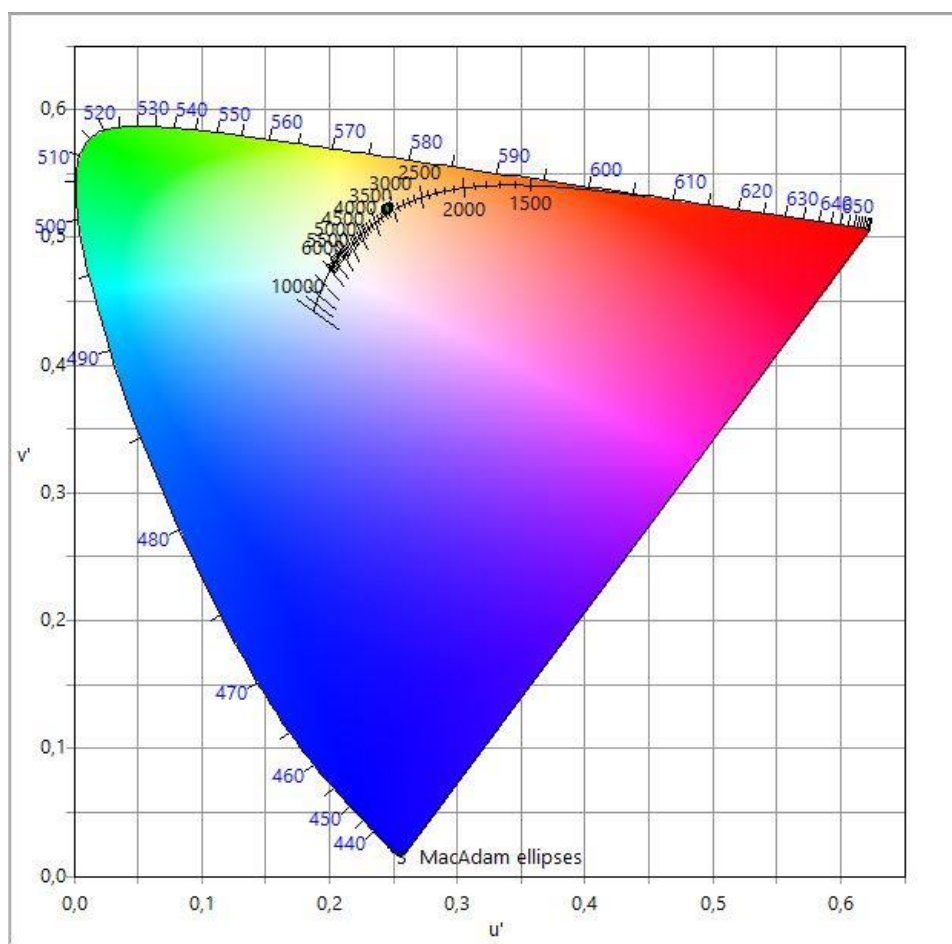


Figure 78 CIE 1976 $u'v'$ plot spectrascan

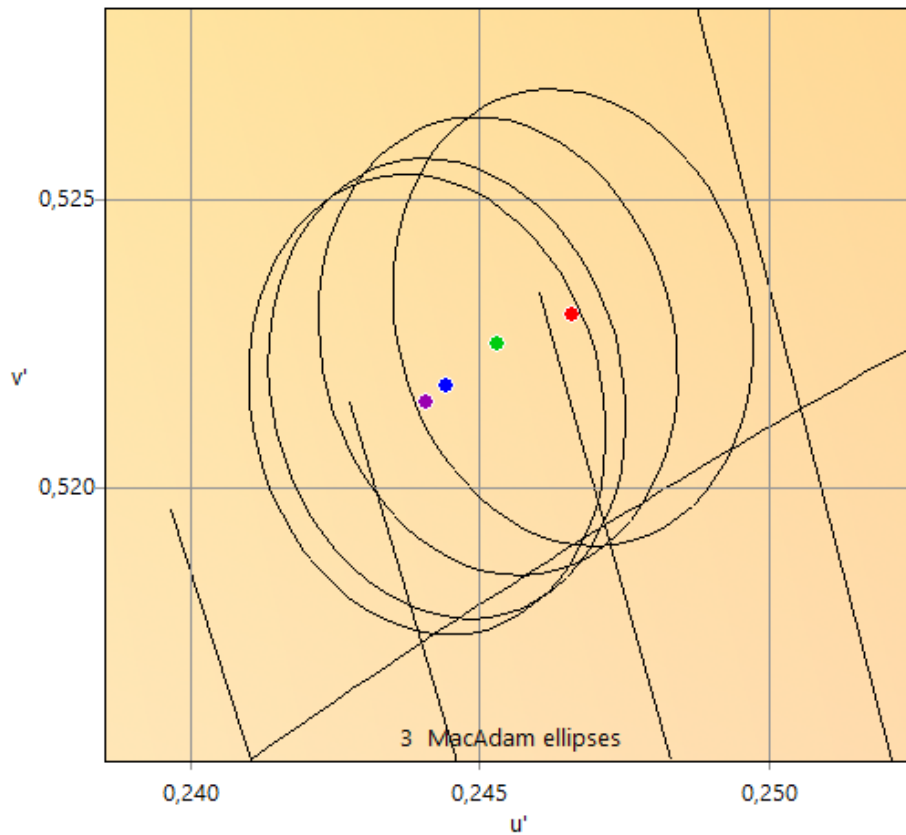


Figure 79 CIE 1976 $u'v'$ zoomed plot spectroradiometer

Figure 80 shows the calculated $u'v'$ values for the measurements with the portable measurement equipment. Figure 81 show the chromaticity diagram and Figure 82 show a more zoomed in version of the same diagram.

| | x | y | u' | v' | CCT | D_{uv} | $D_{u'v'}$ | Point symbol |
|---|--------|--------|--------|--------|------|----------|------------|--------------|
| 1 | 0.4619 | 0.4173 | 0,2608 | 0,5302 | 2723 | 0,0023 | 0,0033 | ● |
| 2 | 0.4615 | 0.4174 | 0,2605 | 0,5302 | 2730 | 0,0024 | 0,0034 | ● |
| 3 | 0.4613 | 0.4174 | 0,2604 | 0,5301 | 2732 | 0,0024 | 0,0035 | ● |
| 4 | 0.4616 | 0.4178 | 0,2604 | 0,5303 | 2731 | 0,0025 | 0,0036 | ● |

Figure 80 CIE 1976 $u'v'$ data from the portable measurement equipment

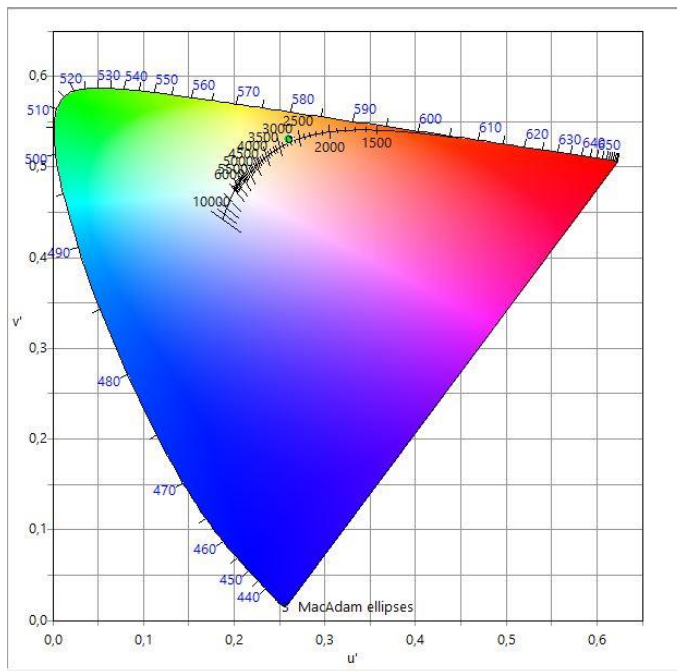


Figure 81 CIE 1976 $u'v'$ plot portable measurement equipment

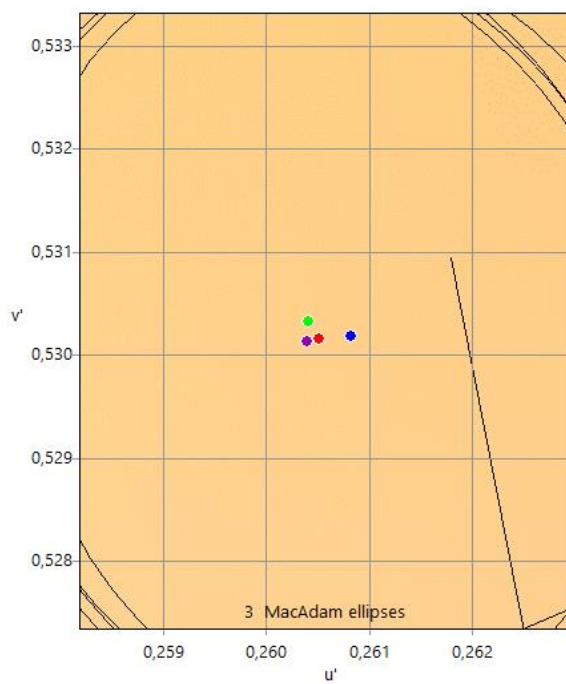


Figure 82 CIE 1976 $u'v'$ zoomed plot portable measurement equipment

6.8.5 Discussion

As can be seen in Figure 54, the soft car target has physically changed a lot. The shell is covered with scratches and the chassis has become difficult to put together as the Velcro tape has become worn out so that it does not stick when trying to attach it.

6.8.5.1 Reflectance

The reflectance of the different sides has not changed significantly. Some of the sides shows a few percent deterioration, but the results of measurements do differ a lot, which indicates some uncertainty in the measurement results. This is valid for the measurements in the IR wavelengths as well. This is most probably caused by salt and other pollution on the 3D soft car target. But the conclusion is that the reflectance has not changed significantly.

6.8.5.2 RGB response

The values for the RGB response for the different sides changes significantly between measurements. The cause is possibly due to a lot of salt and other pollution has contaminated the target and affected the measurements. The conclusion is that it seems like the RGB response has not changed significantly after the tests. The RGB response has deteriorated by a few percent but in comparison to the 100 crashes done it is not a large difference.

6.8.5.3 u'v' chromaticity

The u'v' values for the different measurements change very little. The biggest difference between measurements are 0.0030 in u' and 0.0015 in v', which are very small differences. This means the colour of the 3D soft car target has not changed very much.

6.8.6 Conclusions

The results show that the 3D soft car targets optical characteristics had not changed due to extensive use, using the selected measurement method. Some small changes have been observed but these small changes will not have any effect on the sensors trying to detect the target and therefore the target should still be ok to use from an optical standpoint.

6.9 Results from Geometrical Measurements

6.9.1 Scope of the geometrical study

During the project three different models of SCT's have been studied. The older version of DRI (new and used), DRI360 and 4a. They are all based upon the characteristics of a Ford Fiesta model year 2011. So, for comparison reason a real car is also part of the study. Figure 83-87 below shows the scan data.

The geometrical part of the project comprises of four different aspects:

- Differences between SCT models and real car.
- Variations of same SCT model due to assembly.
- Variations of same SCT due to ageing.
- Alternative measurement system



Figure 83 The real Ford Fiesta 2011 (point cloud)



Figure 84 Old version of DRI - used (point cloud)



Figure 85 Old version of DRI - new (point cloud)



Figure 86 DRI360 (point cloud)



Figure 87 4a (point cloud)

6.9.2 Differences between SCT models and a real car

The studied SCT's are similar but not identical in shape or dimensions. The standard ISO 19206-3 has no defined requirements regarding the static dimensions of the car body. There are, however, requirements regarding dynamics aspects down to 10 mm.

There is no nominal data of the car body. Therefore, no absolute checking has been carried out in this project.

For comparison reasons the data from the full scan of the real Ford Fiesta has been used as reference. The scan data from the SCT's has then been aligned using best fit. This alignment approach is rough but helps visualizing the differences.

Clipping planes in interesting directions are presented in Figure 88 and Figure 89. The impact of these differences in a real test is not part of the project.

6.9.2.1 Longitudinal profile

The longitudinal profile shows some noticeable differences according to Figure 88 below. The DRI (both old and new model) has a higher profile at the back, whilst the 4a target has a lower profile at the back and front.

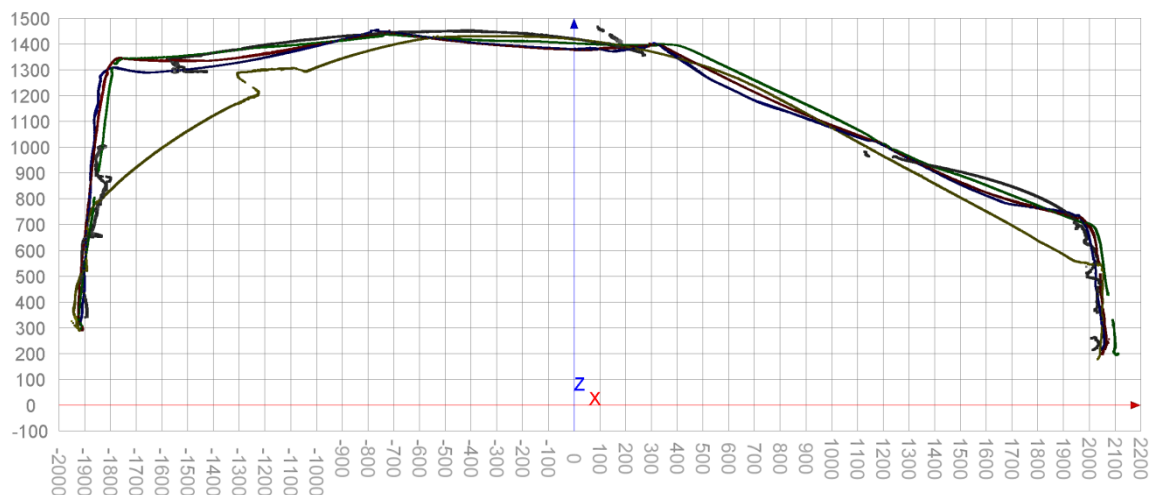


Figure 88 Longitudinal profile of real car and SCT's (scale in mm)

6.9.2.2 Transverse profile

The transverse profile shows minor differences according to Figure 89 below.

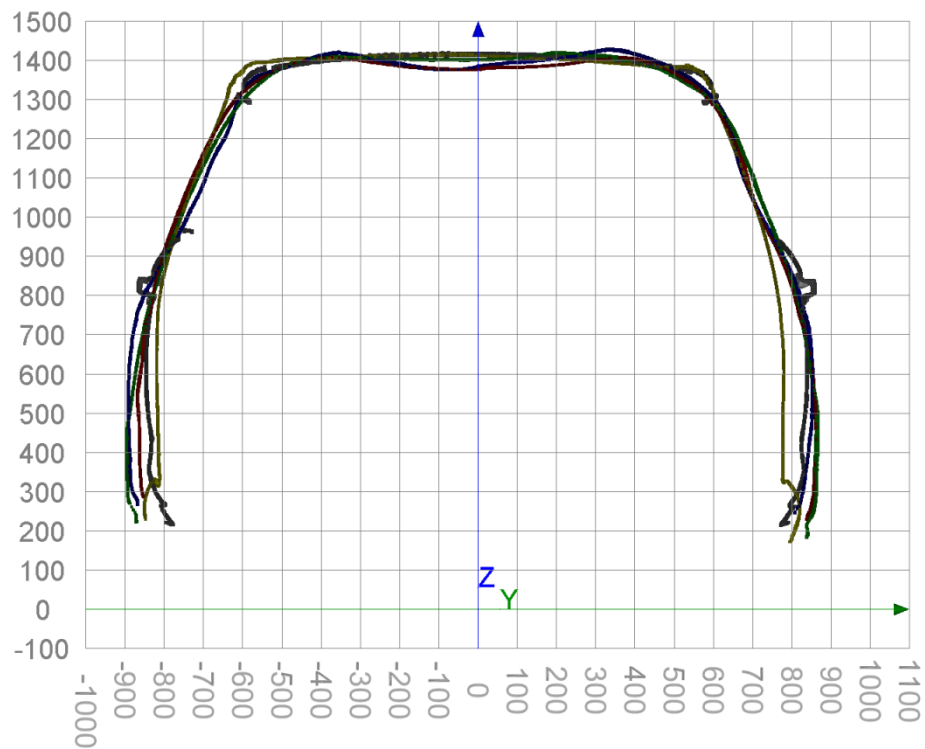


Figure 89 Transverse profile of real car and SCT's (scale in mm)

6.9.3 Variations due to assembly

One of the main purposes of the geometrical part in this project has been to study the variations due to assembly. Consistency in shape and dimension is believed to have a great impact in a real test scenario.

In order to keep the study close to practical use, each SCT was mounted "as instructed".

6.9.3.1 Assembly of used DRI

This SCT has been in use at AstaZero. It showed clear signs of wear & tear. The SCT was assembled and fully scanned 3 times. AstaZero's carrier was used as support. Figure 90 and Figure 91 shows a comparison between first and second and third assembly.

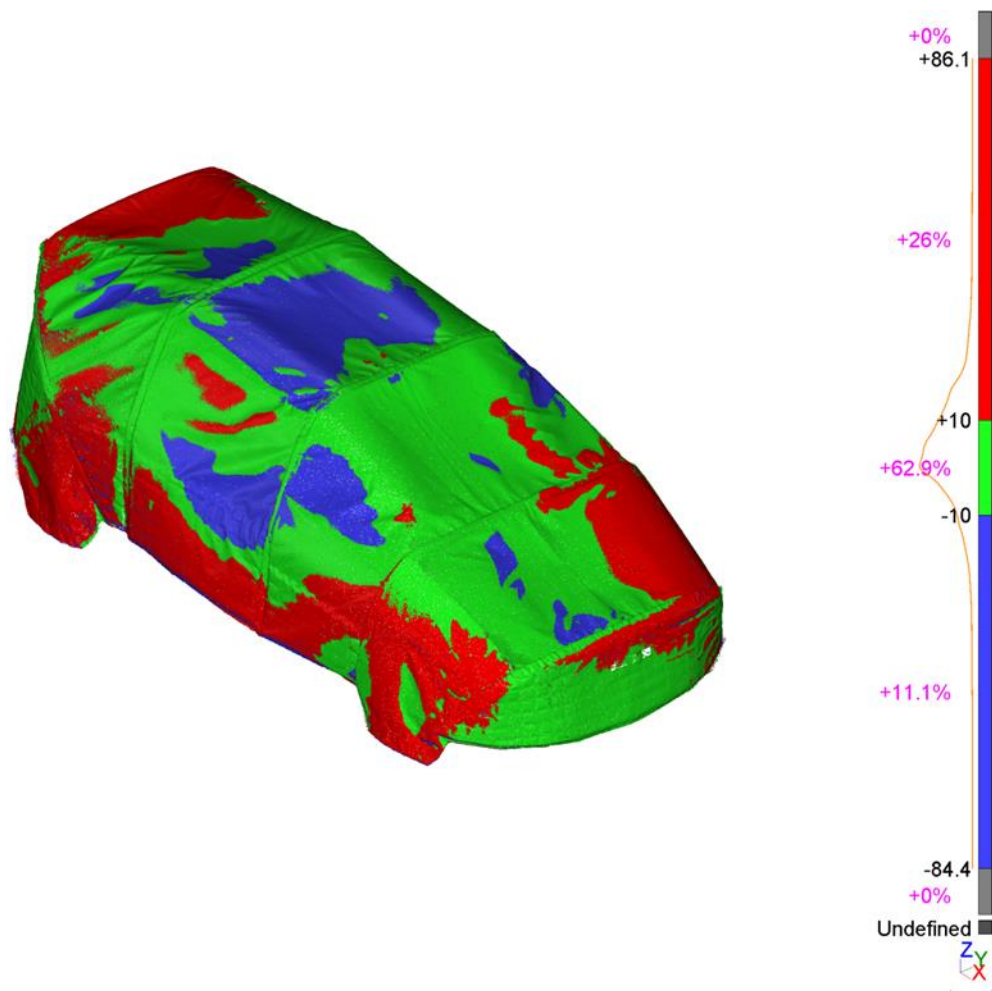


Figure 90 Comparison of first and second assembly, used DRI (result in mm)

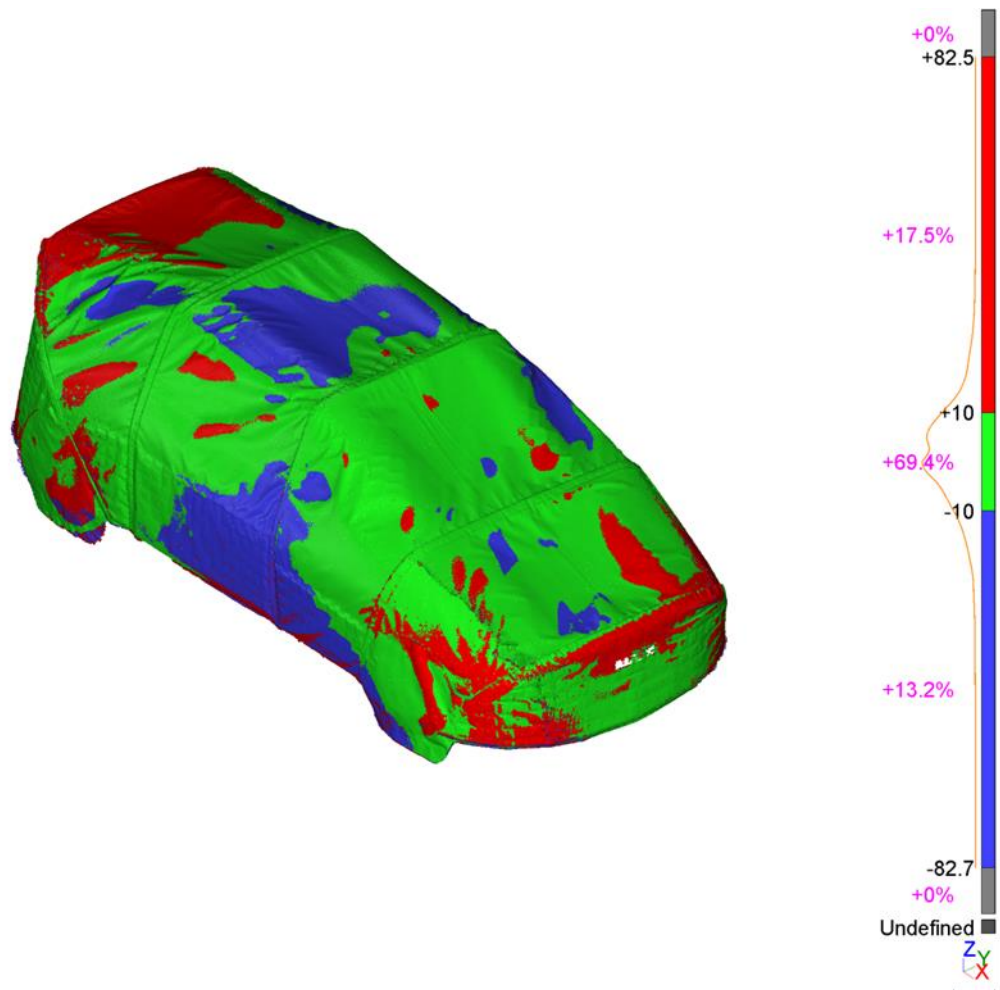


Figure 91 Comparison of first and third assembly, used DRI (result in mm)

Larger variations are found on all parts of the SCT.

6.9.3.2 Assembly of new DRI

This SCT was completely new. The SCT was assembled and fully scanned 3 times. Veoneer's carrier was used as support. Figure 92 and Figure 93 shows a comparison between first and second and third assembly.

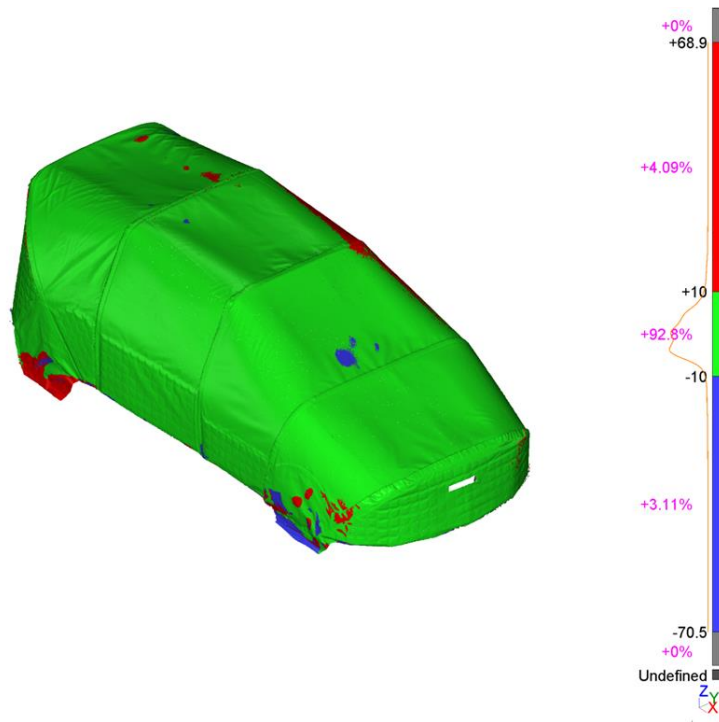


Figure 92 Comparison of first and second assembly, new DRI (result in mm)

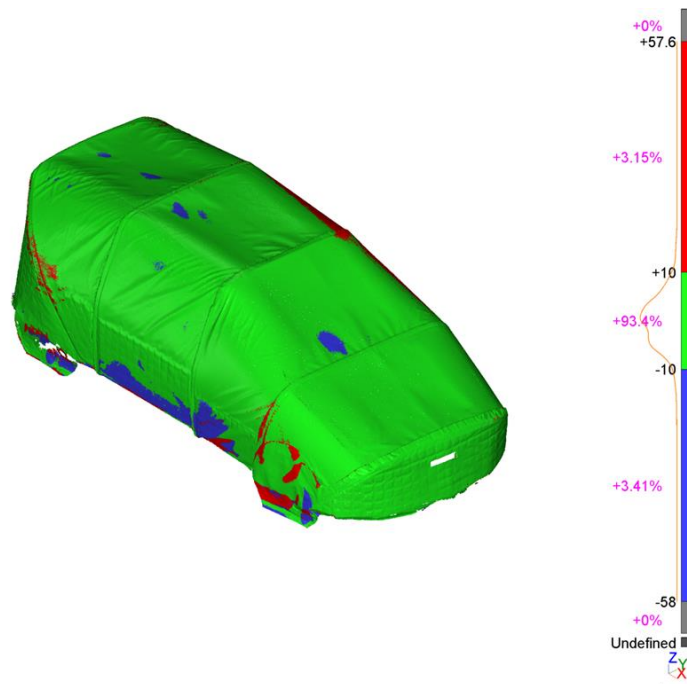


Figure 93 Comparison of first and third assembly, new DRI (result in mm)

Larger variations are found on lower parts of the SCT.

6.9.3.3 Assembly of DRI360

This SCT was completely new. The SCT was assembled and fully scanned 3 times. The support system was placed on car wheel dollies. Figure 94 and Figure 95 shows a comparison between first and second and third assembly.

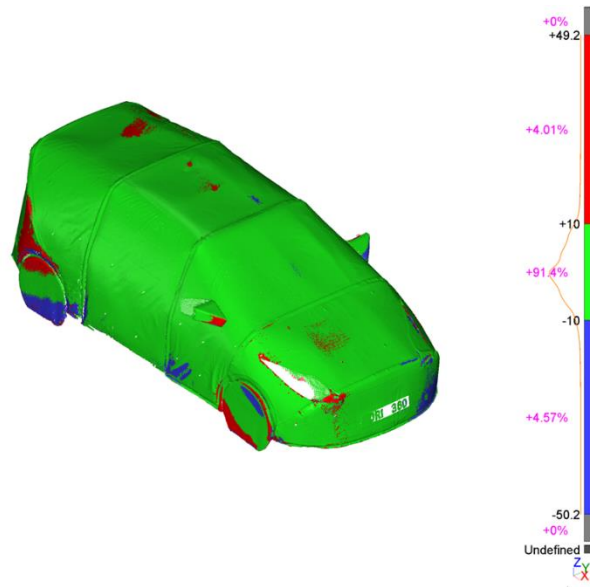


Figure 94 Comparison of first and second assembly, DRI360 (result in mm)

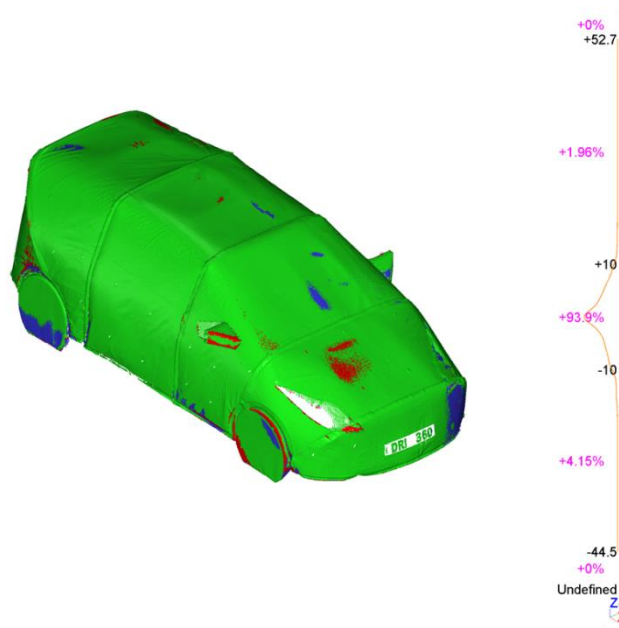


Figure 95 Comparison of first and third assembly, DRI360 (result in mm)

Larger variations are found on separate parts of the SCT.

6.9.3.4 Assembly of 4a

This SCT was completely new. The SCT was assembled and fully scanned 5 times. The support system was placed on the ground. Figure 96 to Figure 99 shows a comparison between assembly 1 and 2 to 5 respectively.

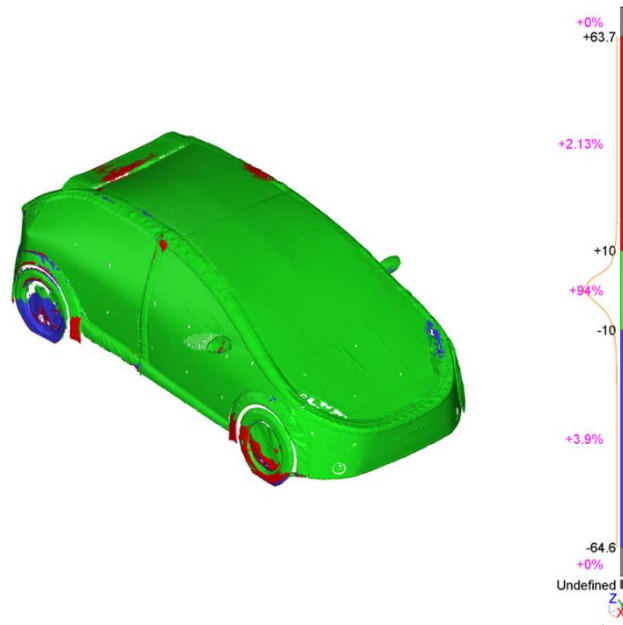


Figure 96 Comparison of assembly 1 and 2, 4a (result in mm)

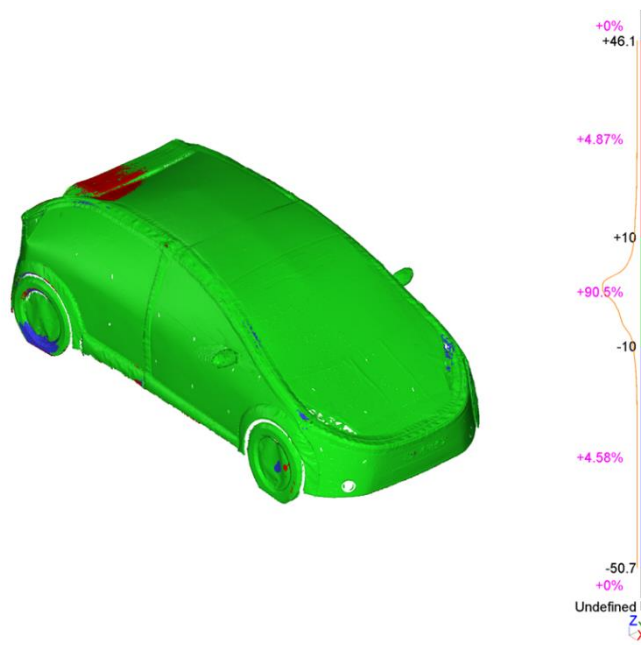


Figure 97 Comparison of assembly 1 and 3, 4a (result in mm)

Larger variations are found on separate parts of the SCT.

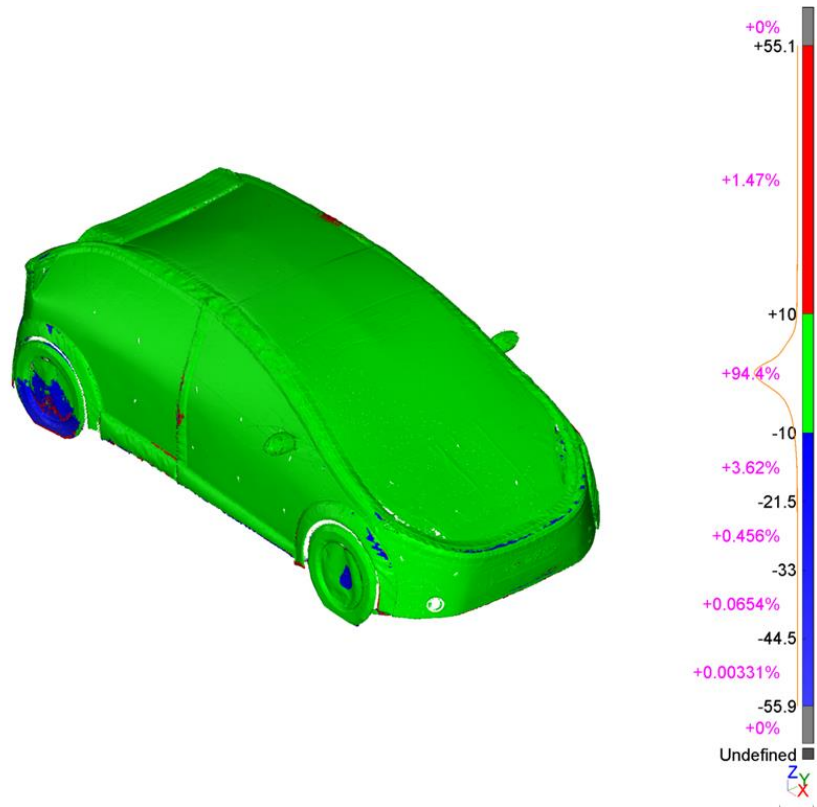


Figure 98 Comparison of assembly 1 and 4, 4a (result in mm)

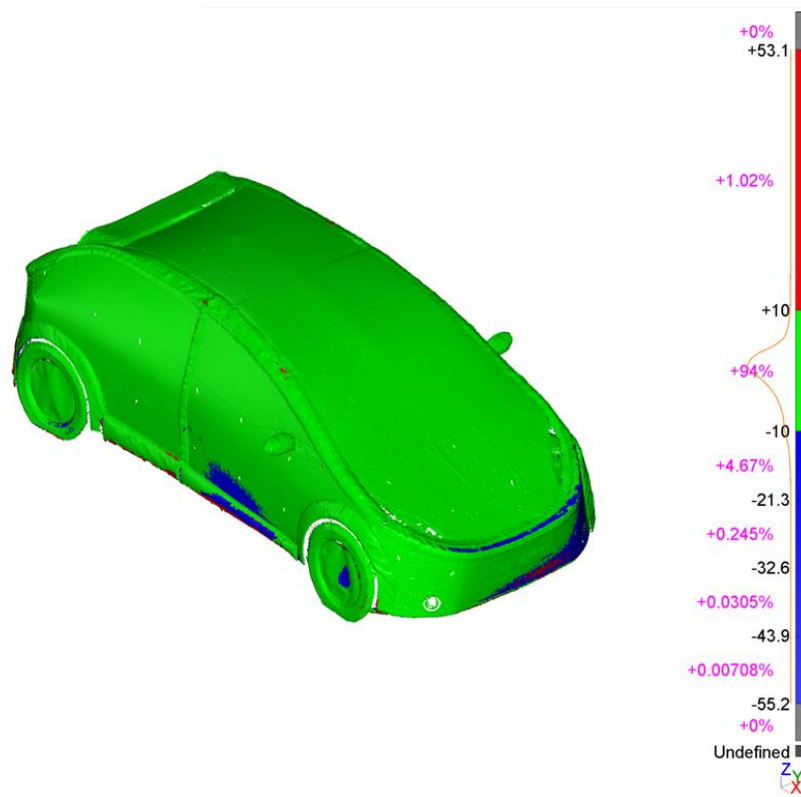


Figure 99 Comparison of assembly 1 and 5, 4a (result in mm)

6.9.4 Variations due to Ageing

As a SCT is used it will most likely degenerate to some extent. Especially if it involves crashes. This part of the project focuses on how the shape varies during accelerated ageing. The SCT (new DRI, same individual as described in 3.2) was crashed in 2 campaigns. The first campaign was carried out at Veoneer in Vårgårda and consisted of 5 crashes. The second was carried out at AstaZero and consisted of 100 crashes.

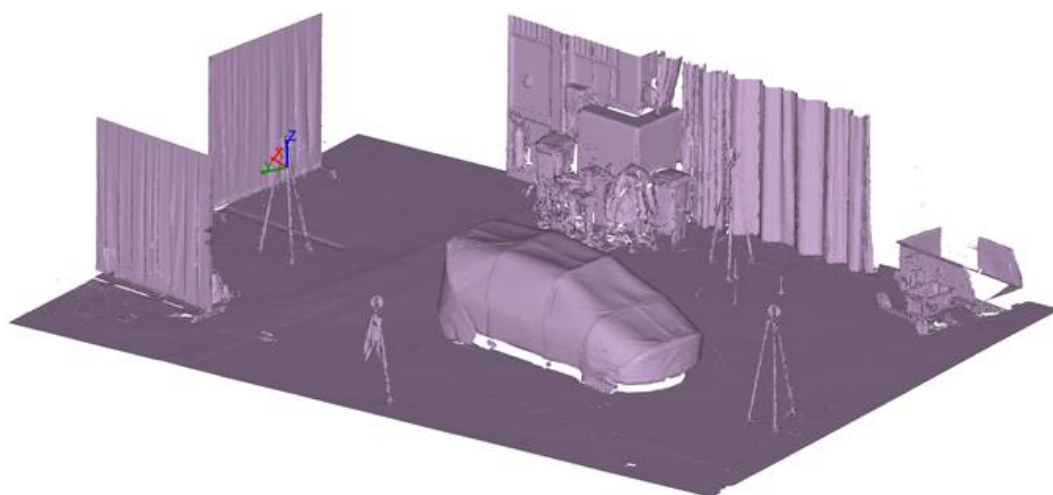


Figure 100 Setup at Veoneer

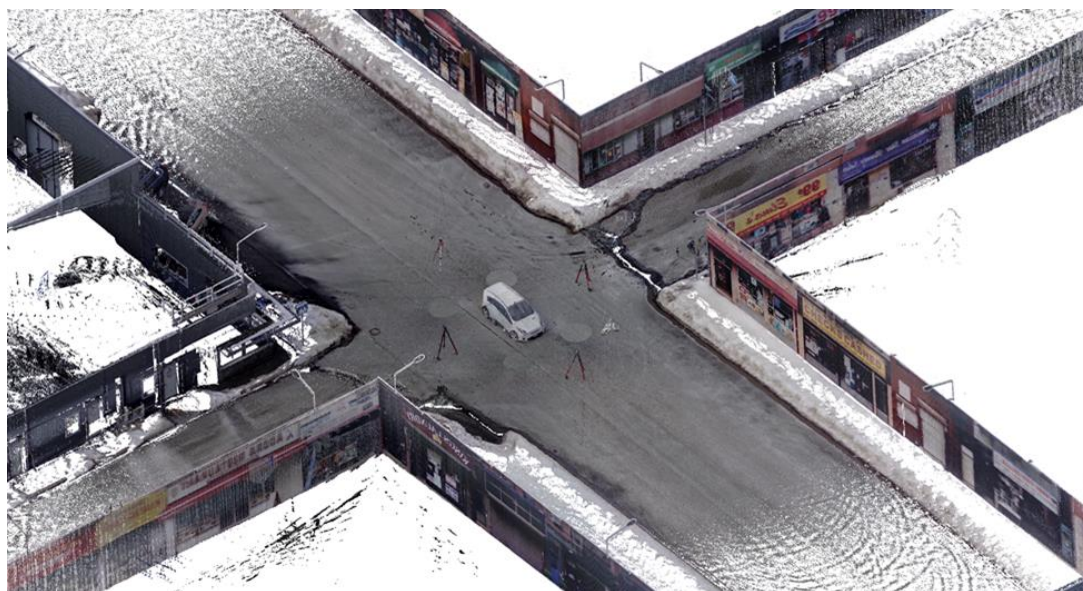


Figure 101 Setup at AstaZero

6.9.4.1 Ageing campaign 1 - Veoneer

This SCT was assembled indoors mounted with its support system on pallets. A first scan was carried out prior to the crashes and a second after. A comparison between first and second scan is shown in Figure 102.

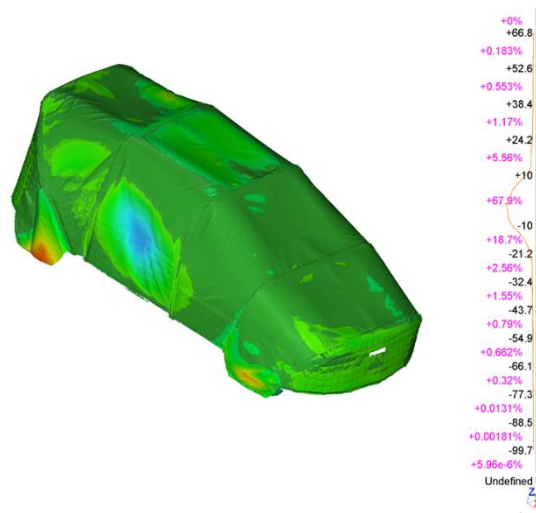


Figure 102 After initial 5 crashes at Veoneer

6.9.4.2 Ageing campaign 2 - AstaZero

This SCT was assembled outdoors mounted with its support system on the ground. A comparison between the initial scan at Veoneer and the scans at different stages at AstaZero is shown in Figure 103 - Figure 107.

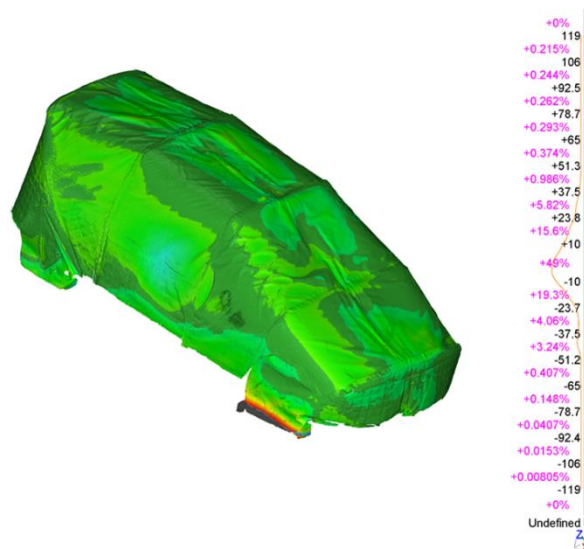


Figure 103 Prior to the first crash at AstaZero

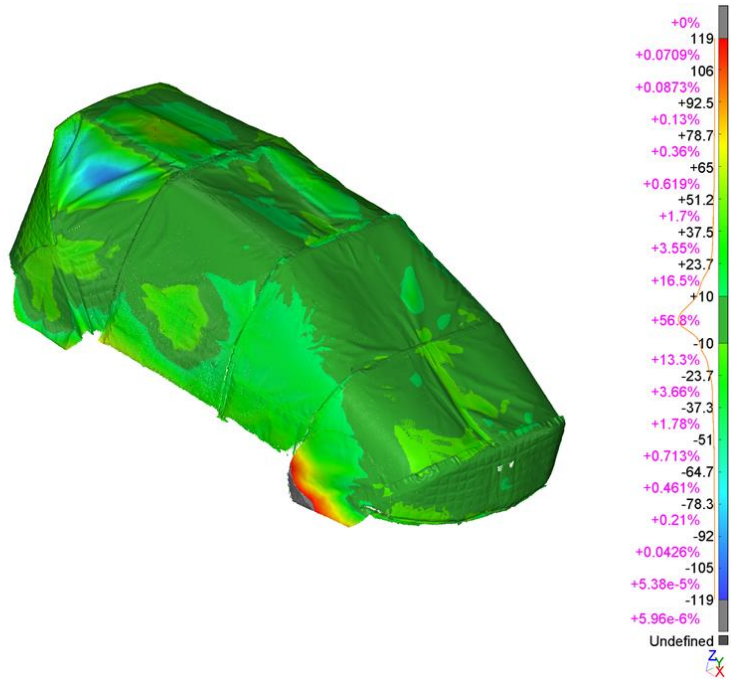


Figure 104 After crash no 21 at AstaZero

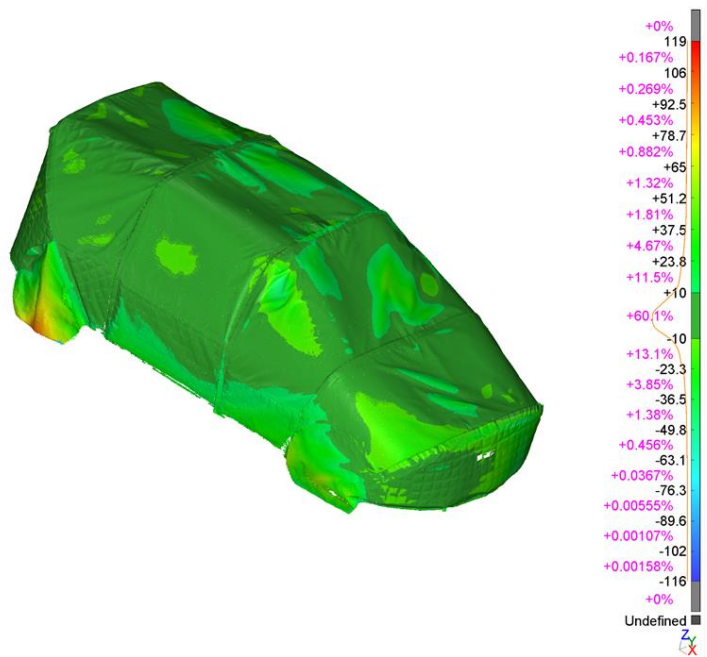


Figure 105 After crash no 51 at AstaZero

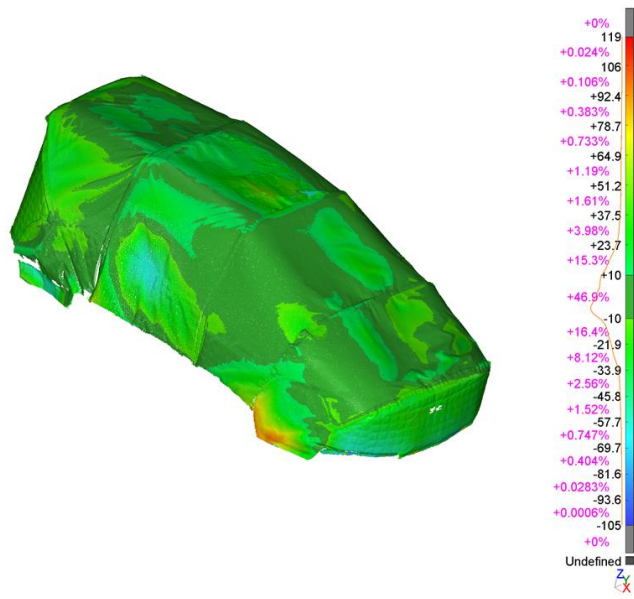


Figure 106 After crash no 75 at AstaZero

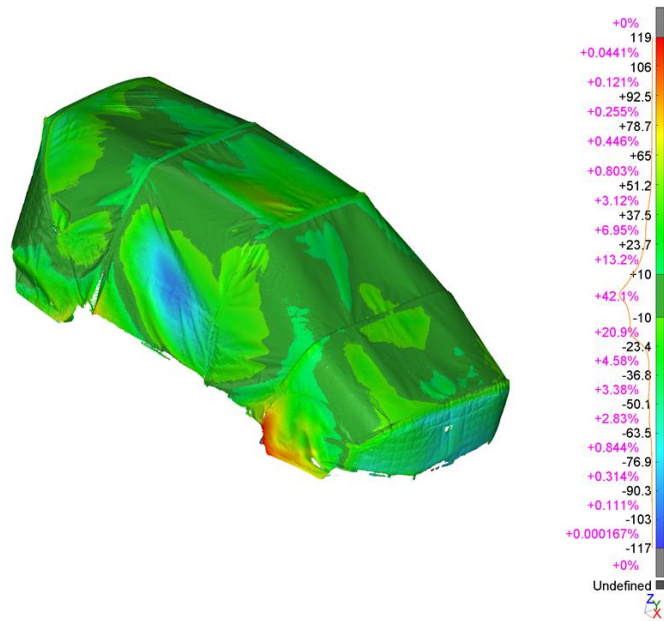


Figure 107 After last crash (no 100) at AstaZero

6.9.5 Conclusions

Because of the nature of the target, it is difficult to define the shape and dimensions with precision. The need to define absolute dimensions is probably not very important. To know that the SCT “looks the same” after re-assembly or a crash is probably of greater importance.

The study shows static variations way beyond what is required dynamically in ISO 19206-3.

Test shows assembly variations up to 80 mm.

Test shows wear & tear up to 120 mm.

To minimize static variations, it is important to use the same support system. And obviously, it is of great importance to take care during assembly. Especially, and common for all models, are the positioning of smaller, separate parts.

Test shows that only a few crashes may considerably alter the main body geometry.

6.9.6 Alternative methods

Based on the results from the initial tests, alternative methods to capture the spatial data of a SCT could be possible. The variation of the first assembly test showed no need for the best precision. A device that allowed for simpler and faster measurement would perhaps be good enough. Not that many alternatives to match size/accuracy/simplicity exists. One plausible device was the DPI8X. It was chosen because it is widely used for other industrial applications. The ordered device showed up in time for the second assembly campaign (DRI360 and 4a).

After initial verification of accuracy and test of workflow it was used to measure the SCT's at the same time it was laser scanned (indoor, good conditions). In total there was 7 comparisons. Figure 26 shows the comparison with the largest deviations.

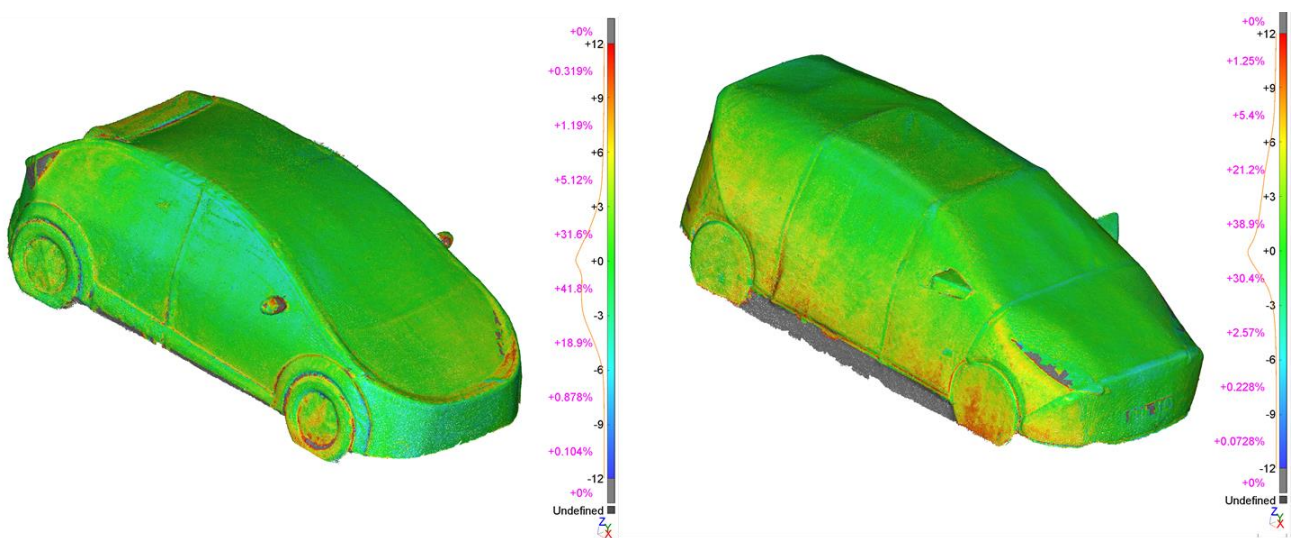


Figure 108 Comparison between laserscan and DPI8X

The tests show deviations up to approximately 10 mm.

Test were also carried out during the second ageing campaign (AstaZero, outdoor winter). These failed. Due to low temperature, snow and other lighting conditions it was not possible to get descent results. Additional test showed however that it worked with no problem under roof cover (better lighting conditions).

The conclusion from all these tests is that the device can capture the spatial data needed under fairly good conditions. It is simpler and quicker to use than an ordinary laser scan, and it is also a single handheld device. At this point there is no built-in application which can be used to compare different static setups. Which means there is no easy “go/no-go” solution.

6.10 Results Volvo Car Tests

6.10.1 Scope of the VCC tests

The tests with the VCC equipment were performed to check how the performance of the vehicle's active safety functions are affected while the geometrical and optical characteristics of the target are changing before and after the 100 crashes.

6.10.2 Test conditions

In this subsection we present the background of the test conditions because the two set of tests were performed in different days.

In Figure 109, we see the test environment in the beginning of the accelerating campaign while the GVT is not crashed. The rear bumper and the wheels are almost no distinguished from the asphalt due to the cloudy weather. In Figure 110 we can see the test environment the day after the 100 crashes on the target and in this case we see clearly the shape of the car and its shadow. The weather is a factor that is not possible to keep the same during the two different days and it can partly enhance or diminish the results.

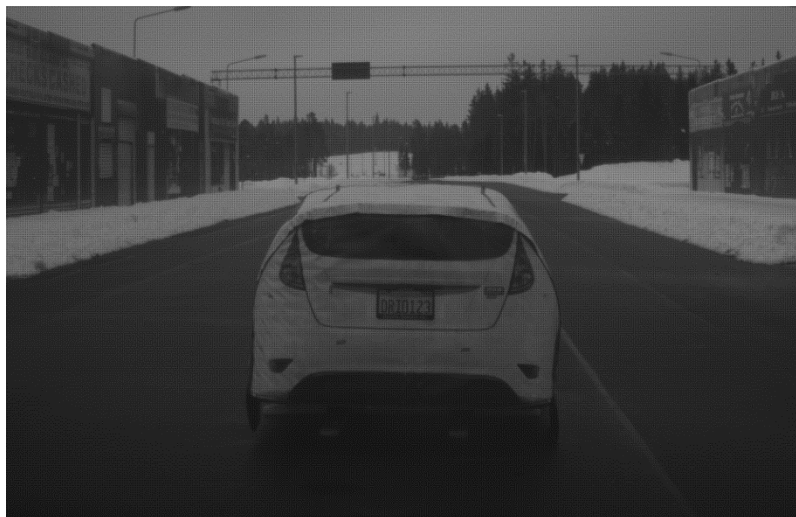


Figure 109 Test environment before the crashes

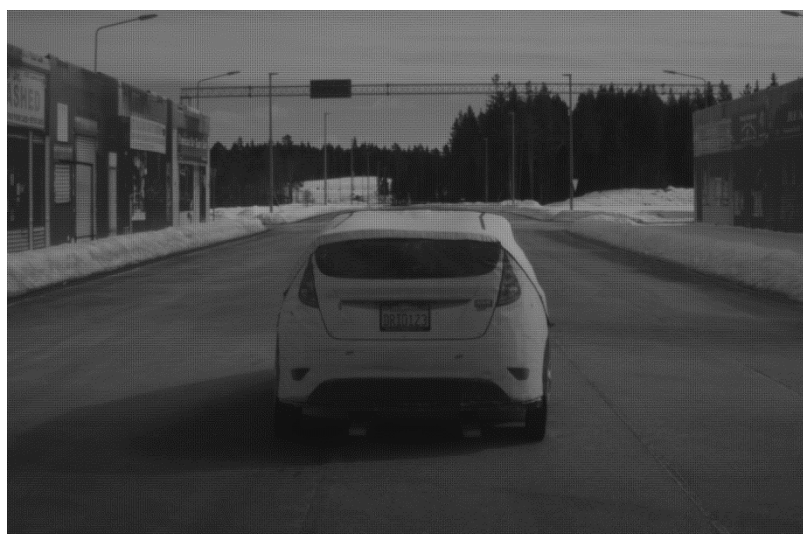


Figure 110 Test environment after the 100 crashes

6.10.3 Analytical results

After the data collection in the AstaZero test track during the accelerating ageing campaign, the data was analysed, and the results are summarized in the next tables. The analysis is based on the confidence levels from the VCC camera as well as on the functions' performance.

The camera reports different confidence levels for the GVT. It reports a low confidence when there is uncertainty about the state estimates of the target (like lateral position of the GVT in regard to the host vehicle) and a high confidence when there is certainty about them.

The focus of the analysis is on when the confidence changes, from low to high and from high to low, while we are approaching the GVT. In addition to the confidence change, we check the performance of the active safety functions, so if the car brakes towards the GVT or if it collides with it.

Below we see the results from the tests while the GVT was new and before we crash into it. The Table 5 shows the results from the rear scenarios while the Table 6 shows the results from the front scenarios.

The column "result" shows the result of the active safety functions and the last column shows the TTC (Time To Collision) when the confidence becomes high.

Note that the TTC values are normalized to the minimum TTC and do not correspond to the original values, for confidential reasons.

| Rear side | | | |
|-----------|------------------|-----------|-------------------------------------|
| Log Name | Host speed (kph) | Result | TTC (s)* when confidence [Low→High] |
| Log 1 | 10 | Avoidance | 1,33 |
| Log 2 | 10 | Avoidance | 1,38 |
| Log 3 | 10 | Avoidance | 1,31 |
| Log 4 | 20 | Avoidance | 1,36 |
| Log 5 | 20 | Avoidance | 1,43 |
| Log 6 | 20 | Avoidance | 1,41 |

Table 5 Before the crashes - Rear scenario

| Front side | | | |
|------------|------------------|-----------|-------------------------------------|
| Log Name | Host speed (kph) | Result | TTC (s)* when confidence [Low→High] |
| Log 7 | 10 | Avoidance | 1,17 |
| Log 8 | 10 | Collision | 1 |
| Log 9 | 10 | Avoidance | 1,42 |
| Log 10 | 20 | Avoidance | 1,44 |
| Log 11 | 20 | Avoidance | 1,33 |
| Log 12 | 20 | Avoidance | 1,41 |

Table 6 Before the crashes - Front scenario

The Table 7 and Table 8 show the corresponding scenarios after the 100 crashes to the target. These two tables include another column which shows if the confidence has dropped from high to low level as well as the number of the drops. Table 5 and Table 6 do not include this specific column because there were no drops.

| Rear side | | | | |
|-----------|------------------|-----------|-------------------------------------|------------------|
| Log Name | Host speed (kph) | Result | TTC (s)* when confidence [Low→High] | Drops [High→Low] |
| Log 1 | 10 | Avoidance | 1,32 | 1 |
| Log 2 | 10 | Avoidance | 1,29 | 1 |
| Log 3 | 10 | Avoidance | 1,37 | 0 |
| Log 4 | 20 | Avoidance | 1,35 | 0 |
| Log 5 | 20 | Avoidance | 1,43 | 0 |
| Log 6 | 20 | Avoidance | 1,38 | 0 |

Table 7 After 100 crashes – Rear scenario

| Front side | | | | |
|------------|------------------|-----------|-------------------------------------|-------|
| Log Name | Host speed (kph) | Result | TTC (s)* when confidence [Low→High] | Drops |
| Log 7 | 10 | Avoidance | 1,42 | 0 |
| Log 8 | 10 | Avoidance | 1,45 | 0 |
| Log 9 | 10 | Avoidance | 1,36 | 0 |
| Log 10 | 20 | Avoidance | 1,31 | 1 |
| Log 11 | 20 | Avoidance | 1,38 | 0 |
| Log 12 | 20 | Avoidance | 1,44 | 0 |

Table 8 After 100 crashes – Front scenario

6.10.3.1 Comparison of the same test case two different days

In this case we compare exactly the same test case but in two different days, e.g. the rear scenarios of 10 kph before the crashes with exactly the same scenario after the 100 crashes and we notice that after the 100 crashes in Table 7 and Table 8 there are drops in the confidence which could be because of the “100 times crashed” and damaged target. The appearance of the GVT becomes visually much worse than in the beginning of the tests.

We can see for example how worse it becomes the front side of the target.

The target before the crashes can be seen in Figure 111.



Figure 111 The target before the crashes

The target after the 100 crashes can be seen in Figure 112.



Figure 112 The target after the crashes

It is noticeable that the front side of GVT is much worse after the 100 hits, for example the front bumper, the registration number, the headlights, the windscreen and the connection surfaces and this is one of the main reasons that the drops occurred.

6.10.3.2 Comparison of the same test case at the same day

In this case we compare exactly the same test case at the same day that one set of tests performed. For example, we compare the front side scenario at 10 kph in different repetitions (log 7 and log 8 in Table 6) and we notice a collision. This occurs because of the bad geometry of the car. During the assembly of the car and due to the fact that the human factor is included because different people put together the different parts into the target, the GVT does not look like the same from one crash to another. The Figure 113 corresponds to log 8, where the collision occurred, and we see that the front right wheel is on the air and the left side of the car exceeds to the body of the car with result to see partly the left wheel of the car. This view does not mimic the view of the real car where in real case we never see parts of the wheel while looking the front part of it. This is the reason why the collision happened in this case.



Figure 113 Before the crashes - front scenario

6.10.4 Conclusions

The two ways of comparison of the data conclude to the result that the shape of the target plays an important role to the vision algorithms as well as to the active safety functions' performance. The wrong geometry of the car can deteriorate both. Therefore, it is very important that during the development of new functions while a big amount of sensor data is collected and during the EuroNCAP rating tests the geometry of the car resembles a real car as much as possible.

In addition, the damaged surface with degraded characteristics of the car, for example the registration plate, can affect a lot the test results, but it is difficult to measure how much based on the confidence analysis, especially because factors like the weather can also affect the performance.

6.11 Results from Veoneer tests

6.11.1 Veoneer Mono-vision Camera

6.11.1.1 Purpose

To investigate the effect upon classification performance of the mono-vision camera to a 3D vehicle target, because of accumulated wear and tear from days of repeated impacts on the target.

6.11.1.2 Methods

A Mercedes test vehicle equipped with a Veoneer stereo-vision camera was used to record the raw data. One camera channel was then used to provide the data to the Mono-vision classifiers. The vehicle was used to record the first 41 impacts of the 3D Target. The vehicle speed at impact was 50km/hr for every test, and the overlapping of the impact between the 2 vehicles ranged from 50%-100%, with 100% being the centre points of both vehicles meeting at the same point. The recorded sequences were analysed using the Veoneer Mono-Vision system for GVP4, and the simulations and visualizations were built from the FdMainAes development branch SHA-id c361c17. The classifier tested was for the rear-end of the vehicle.

6.11.1.3 Results and Analysis

The focus of the analysis was to see how well the classifiers performed during the testing. The classifiers are used to determine if an object in the field of view of the camera is a car, truck, etc. The bounding boxes visualized from the recorded data are classification candidates output by the classifiers in GVP4, in which, yellow boxes are cars, and blue boxes are trucks. The 41 recordings were then analyzed to determine the classification performance of each run and to determine if the performance decreased over time. The classifier showed good performance from the first impact to the last impact.

6.11.1.4 Conclusions

The 3D target is classified as a vehicle by the GVP4 classifiers throughout the recorded sequences. The tests also indicate that the 3D Target has good enough quality for the GVP4 vision system after the wear and tear introduced during this testing.

6.11.2 Veoneer 77 GHz Radar

6.11.2.1 Purpose

To investigate if the Radar Cross Section (RCS) of the 3D target changes over time, because of accumulated wear and tear from days of repeated impacts on the target.

6.11.2.2 Methods

A Veoneer 77 GHz Multimode radar, on a radar cart (See Figure 114) and measuring methods (See Figure 115) developed within the HiFi Radar target project, was used to measure the RCS of a 3D vehicle target after repeated impacts. The target was measured after every 10 or so impacts, with a total of 100 impacts being performed.

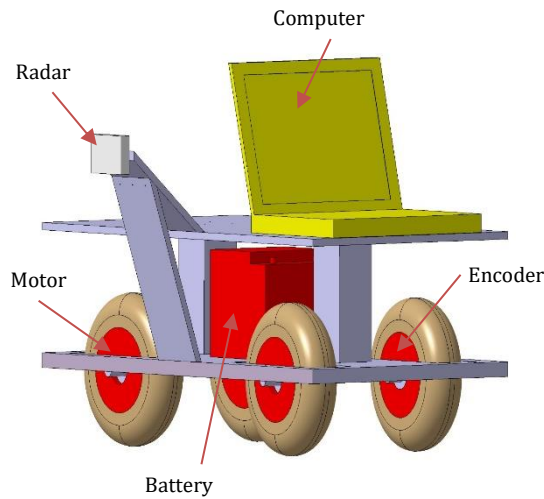
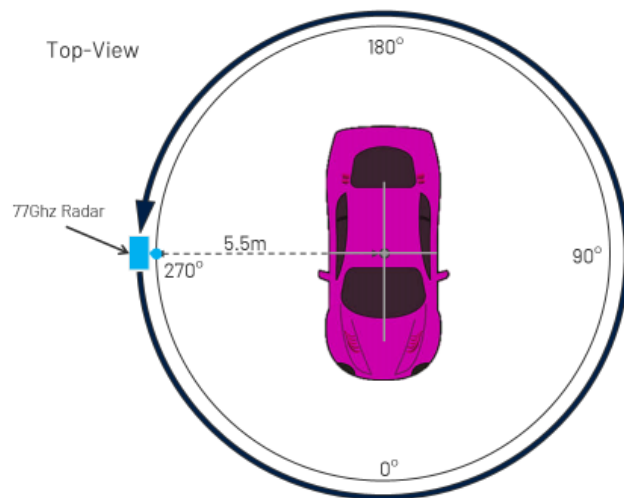


Figure 114 – Radar Cart

veoneer

Vehicle Measurement:

- Continuous circular 360° Rotation around the vehicle center point
- Center defined by ½ vehicle width and ½ wheel base
- Radar distance 5.5 m from center
- Radar height 0.5 m



© 2018 Copyright Veoneer Inc. All Rights Reserved

Figure 115 – Radar cart Measurement method.

6.11.2.3 Results and Analysis

Three Reference measurements were made before the first impact. The target was not moved, rebuilt, or changed during the reference measurements, but the radar cart was moved into place and taken away after each measurement to simulate the normal measurement conditions for the campaign. It can be seen from the plot in Figure 116 that the reference measurements were all very close, with approximately a difference between 0.1 – 2.4 dB/m².

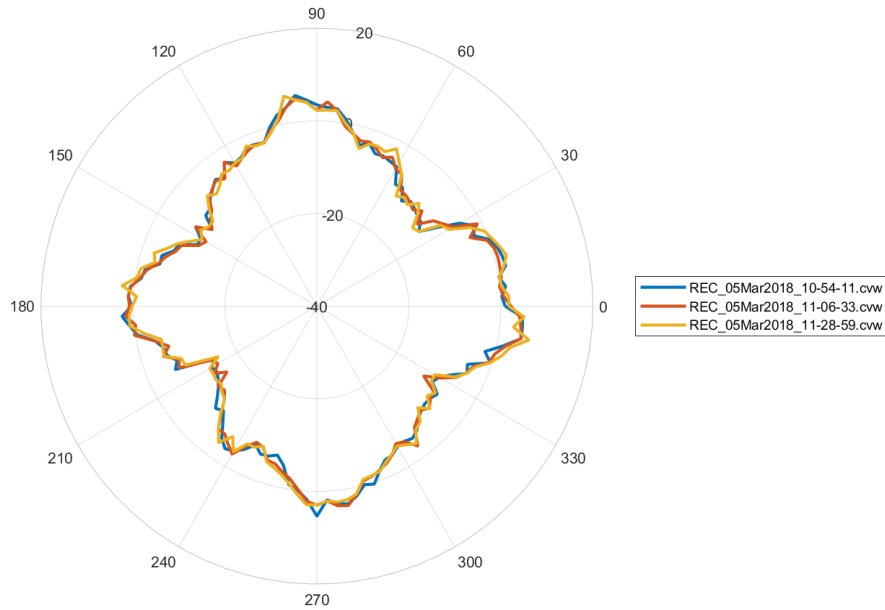


Figure 116

Figure 117 shows the RCS of the 3D target from the 10 measurements along with the 3 reference measurements. It can be seen, that the difference in the measurements is much larger than those of the reference measurements, with an approximate difference between 4-12 dB/m². The biggest change appeared in measurement directly after hit 51.

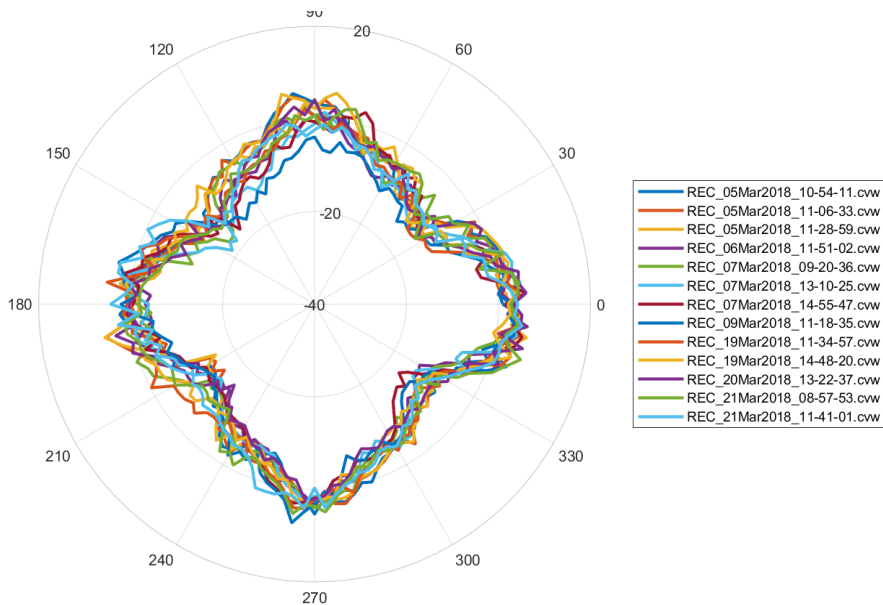


Figure 117 - Radar Measurements

As a comparison we can look at the RCS of real vehicles taken with the radar cart in the Hifi Radar project. 37 vehicles were measured from various manufactures and from various size segments, ranging from mini cars (Segment A) to sport utility vehicles (Segment J). The size of the 3D target would put it in the B-C segments. The plot in Figure 118 shows the min and max RCS as a combination of the 37 measured real vehicles, with an approximate difference between the min and max ranging from 4-16 dB/m². The next plot Figure 119 show the comparison of the two sets of data.

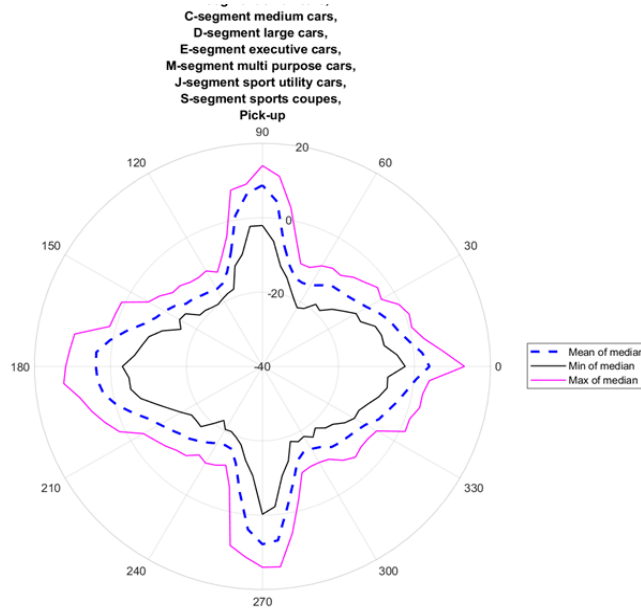


Figure 118 – Min-Max Radar measurements from 37 real vehicles from various car segments

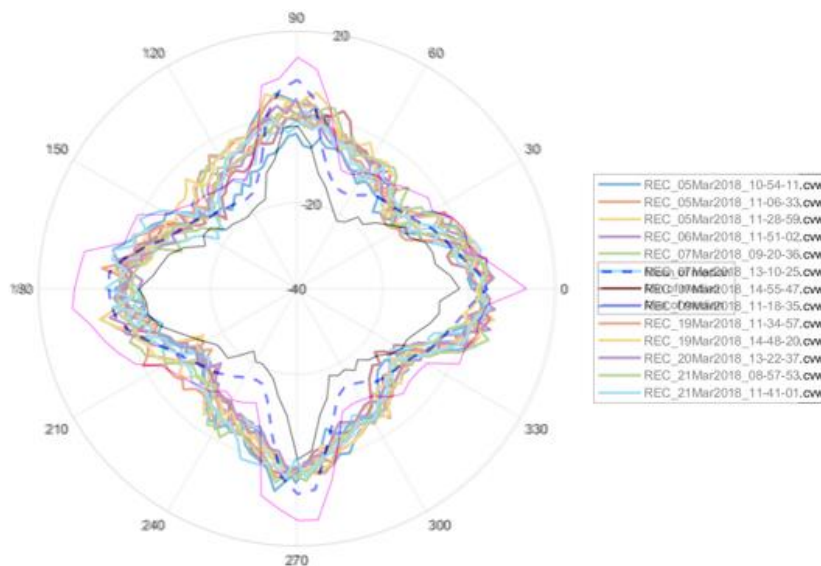


Figure 119 – Comparison Target vs Real vehicles.

6.11.2.4 Conclusions

From the results, it can be seen, that there is difference in the RCS of the 3D target vehicle after each hit and rebuilding of the target. However, it is not conclusive if this difference comes from rebuilding, impact, or some other factor. Also, difference in the RCS of the 3D target is in the range of what you would see from a range of various vehicles, not from what you would see from a single vehicle.

6.12 Delivery to FFI-goals

The FFI goals for the Electronics, Software and Electronics (EMK) program are subdivided in six areas

1. Electrical Architecture – inside the vehicle
2. Architectures outside the vehicle – the connected system
3. Cybersecurity
4. Man-Machine Interaction
5. Verification and Validation
6. Technology for Green, Safe, Automated and Connected Functions

The HiFi Visual Target concerns mainly area 6 - Technology for Green, Safe, Automated and Connected Functions. In the following chapters the goals of these subareas will be compared with what has been achieved in HiFi Visual Target.

FFI-Goal: To develop necessary base technologies on component level in order to realize functions. For “safety functions” and “automated functions” it is primarily control functions including sensor technologies.

HiFi Visual Target delivery: The safety and automated functions will still need to be tested and validated against Euro-NCAP targets to test and benchmark these functions. Optical sensor technologies like e.g. cameras, need to be tested with the 3D soft car target that is standardized for the Euro-NCAP tests. HiFi Visual Target has delivered tools and knowledge that will be useful to secure the validity of the 3D car target from a sensor perspective over time.

6.13 Deliverables and Reports

Several reports and deliverables have been produced within the project. All deliverables except for the Final Report are project internal and not public.

List of deliverables:

- D2.1 Sensor Definition and Optical Characteristics
- D2.2 Definition of Targets
- D2.3 Definition of Measurement Methods and Tools
- D2.4 Measurement Validation Report
- D3.1 Optical Test Setup
- D3.2 Geometrical Test Setup
- D3.3 Measurement Validation Report
- D4.1 Optical characteristics Measurement Report
- D4.2 Geometrical properties Measurement report
- D5.1 Final Seminar
- D5.2 Final Report
- Portable Optical Instrument
- Portable Geometrical Scanning Tool

7 Dissemination and Publications

7.1 Knowledge and Results Dissemination

The project and the results have been presented at internal meetings within each partner's organization and at an external conference (AMAA2017).

At the end of the project, a HiFi Visual Target Final Seminar was held at AstaZero proving ground in June 20th 2018.



Figure 120 Pictures from the Final Seminar at AstaZero.

| How has the project results been, or planned to be, used and spread? | Mark with X | Comment |
|--|-------------|--|
| Increased the knowledge in the area | X | |
| Transfer to other advanced technical development projects | X | Partners are discussing the possibility of a continuation in a new application for a research project. |
| Transfer to product development projects | | |
| Introduced on the market | | |
| To be used in investigations, regulations or political decisions | X | Results fed in to ISO standardization |

HiFi Visual Target has also been cooperating with the HiFi Radar Target projects e.g. by collocating test activities, reusing geometry scanning data for EMC modelling and coordinating the measurements on the 4a 3D car target. The long-term goal for RISE and AstaZero is to continue developing methods and tools to secure the quality of 3D car targets over time. Additionally, the results have also been fed into standardization activities within ISO (ISO/WD 19206-3 Active safety targets - Vehicle 3D targets).

7.2 Publications

- [21] S. Nord, M. Lindgren. "HiFi Visual Target - Methods for Measuring Optical and Geometrical Characteristics of Soft Car Targets for ADAS and AD". Lecture Notes in Mobility: Smart Systems Transforming the Automobile / [ed] Gereon Meyer, Berlin: Springer, 2017, pp. 201-209.
- [20] Characterization of visual and IR reflectivity for soft car targets. Written by Isak Pettersson and Kasper Johansson at Luleå Technical University.

8 Conclusions and Future Research

8.1 Conclusions

HiFi Visual Target has developed, validated and demonstrated measurement methods for optical and geometric properties of soft 3D car targets and contributed to international standardization with methods and results. The results from the measurements with the selected optical method show that the 3D soft car targets optical characteristics had not changed due to extensive use.

When it comes to the geometrical characteristics of the soft 3D target, the nature of the target makes it difficult to define the shape and dimensions with precision. The need to define absolute dimensions is probably not very important. To know that the soft 3D car target “looks the same” after re-assembly or a crash is probably of greater importance. The study shows static variations way beyond what is required dynamically in ISO 19206-3 which implies that the geometrical definitions in the standard should be defined in a better and more concise way.

The results from the tests done by Volvo Cars show that the shape of the target plays an important role to the vision algorithms as well as to the active safety functions’ performance. The wrong geometry of the car can deteriorate both. Therefore, it is very important that during the development of new functions while a big amount of sensor data is collected and during the EuroNCAP rating tests the geometry of the car resembles a real car as much as possible.

In addition to this, the damaged surface with degraded characteristics of the car, for example the registration number, can affect a lot the test results, but it is difficult to measure how much based on the confidence analysis, especially because factors like the weather can also affect the performance.

One important conclusion from the tests is that the optical measurement method outlined in ISO 19206-3 should also include measurements on the soft 3D car target features like e.g. headlights, registration plate etc, and not only the white surfaces, which has been concluded do not deteriorate as much as expected.

8.2 Future Research

The purpose of this section is to provide a list of topics that can serve as input for decisions for future research and development activities. It can e.g. be work that was identified during the project as extensions but had to be put aside for budget and/or resource reasons. It can also be topics that did not fall within the project scope but that still is of importance and interests of the partners and that need further research and development to develop measurement technologies and methods.

- The vast amount of data was not possible to investigate to the full extent within the project. There is a need to continue the analysis of the data to investigate additional aspects.
- The optical measurement method could both be further developed to make it more practical for outdoor measurements and also to include a way to measure on other features as e.g. headlights or registration plate.
- More research could be spent on different measurement angles for the reflectance spectroscopy could be done.
- The handheld geometrical method could also be improved.
- Work on how to better define the geometrical properties of the 3D car target in ISO 19206-3 should also be included in future work.

9 Participating Parties and Contact Persons



Stefan Nord
stefan.nord@ri.se
+46 10 516 5931



John Lang
john.lang@veoneer.com
+46 322 667717



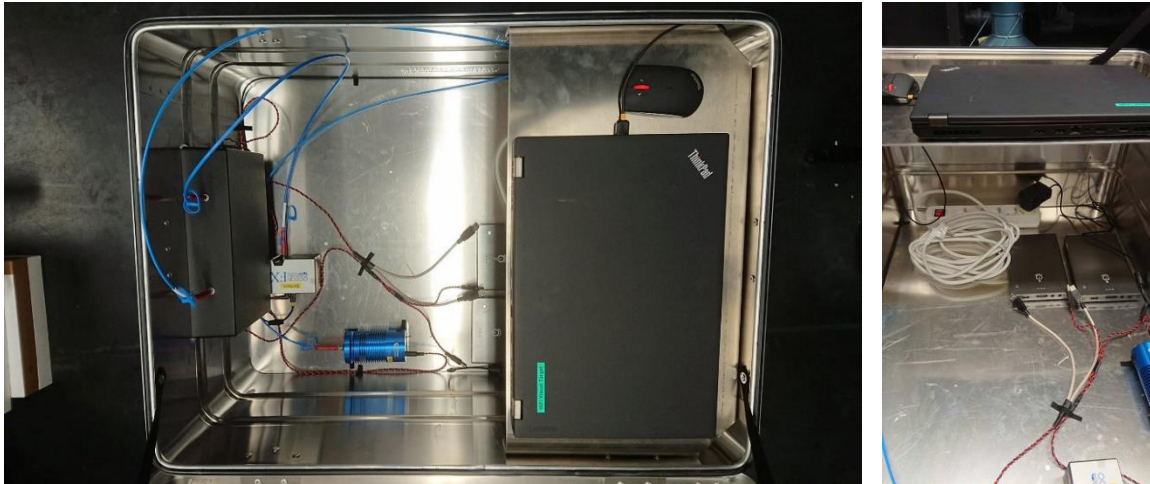
Georgia Diakou
georgia.diakou@volvocars.com
+46 72 9707288

10 References

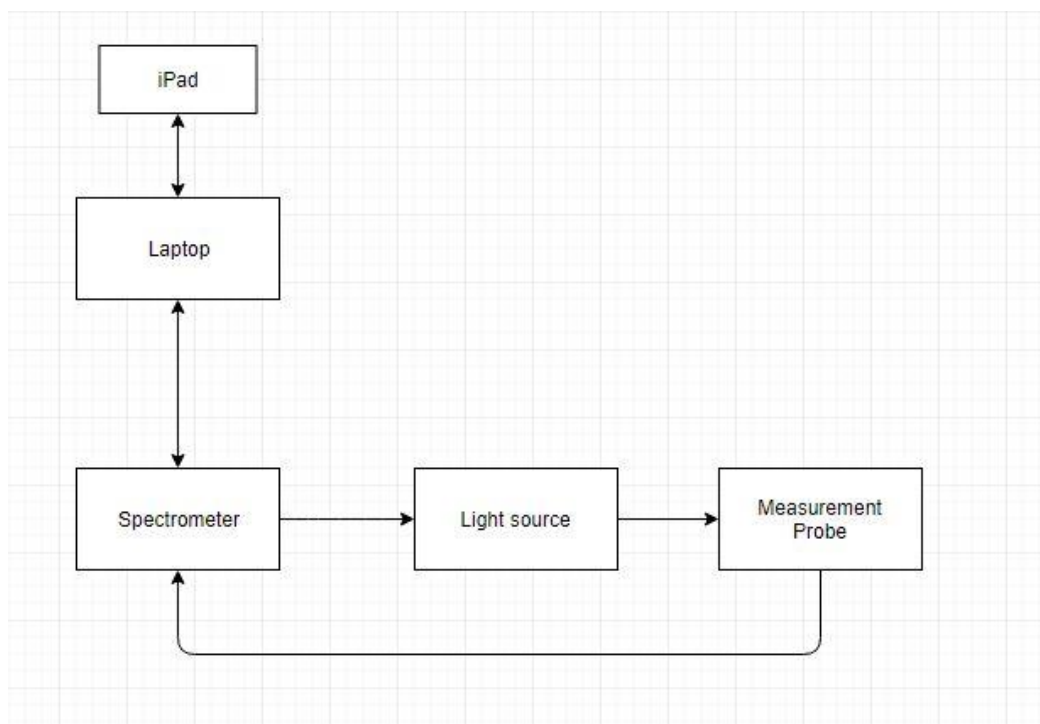
- [1] Volvo Car Corporation leads the way in car safety: risk of being injured in a Volvo reduced by 50 percent since year 2000. Press-release. <https://www.media.volvocars.com/global/en-gb/media/pressreleases/45468>. Accessed on June 11th, 2018.
- [2] I. Isaksson-Hellman, M. Lindman. "Real-World Performance of City Safety Based on Swedish Insurance Data," 24th International Technical Conference on the Enhanced Safety of Vehicles (ESV). No. 15-0121, Gothenburg, Sweden, June 8-11, 2015.
- [3] M. Rabben, R. Henze, and F. Küçükay, "Dynamic Crash Target for the Assessment, Evaluation and Validation of ADAS and Safety Functions". Proc. 3rd International Symposium on Future Active Safety Technology Towards zero traffic accidents, 2015; and references therein.
- [4] V. Sandner, "Development of a Test Target for AEB Systems," 23rd International Technical Conference on the Enhanced Safety of Vehicles (ESV). No. 13-0406, Seoul, Korea, South, May 27-30, 2013.
- [5] Yamada. "Three-Dimensional High Resolution Measurement of Radar Cross-Section for Car in 76 GHz Band", R&D Review of Toyota CRDL Vol. 36 No 2, Toyota Central R&D Labs, Inc., H. Suzuki, "Radar cross section of automobiles for millimeter wave band," JARI research Journal, Vol. 22, No. 10, pp. 475-478, 2000.; N. Yamada, "Radar cross section for pedestrian in 76 GHz," Proceedings of 2005 European Microwave Conference, Vol. 2, 4-6 Oct. 2004, pp.46-51.
- [6] P. Lemment et al, "Evaluation of Pedestrian Targets Used in AEB Testing: A Report from Harmonisation Platform 2 Dealing with Test Equipment," 23rd International Technical Conference on the Enhanced Safety of Vehicles (ESV). No. 13-0124, Seoul, Korea, South, May 27-30, 2013.
- [7] City Safety by Volvo Cars – outstanding crash prevention that is standard in the all-new XC90, press release from 2014, December 5. Available at: <https://www.media.volvocars.com/global/en-gb/media/pressreleases/154717/city-safety-by-volvo-cars-outstanding-crash-prevention-that-is-standard-in-the-all-new-xc90>. Accessed on June 11th, 2018.
- [8] ISO/WD 19206-3 Active safety targets - Vehicle 3D targets - 2016-11-10
- [9] 4A Vehicle Target Specification Version 0.5
- [10] 4activeSystems. n.d. 4activeC2 free standing car target. Accessed 07 04, 2017. <http://www.4activesystems.at/en/products/dummies/4activec2.html>
- [11] 4activeFB autonomous driving platform. Accessed 07 06, 2017. <http://www.4activesystems.at/en/products/test-equipment/4activefb.html>
- [12] Anthony Best Dynamics. "Guided Soft Target - HD." AB Dynamics. Accessed 07 06, 2017. [http://www.abd.uk.com/upload/files/2017-05-25_14-29-27_SP-6012%20Guided%20Soft%20Target%20Heavy%20Duty%20\(GST%20HD\)%20Specification.pdf](http://www.abd.uk.com/upload/files/2017-05-25_14-29-27_SP-6012%20Guided%20Soft%20Target%20Heavy%20Duty%20(GST%20HD)%20Specification.pdf)
- [13] "Guided Soft Target." AB Dynamics. Accessed 07 06, 2017. [http://www.abd.uk.com/upload/files/2017-05-25_14-28-50_SP-6011%20Guided%20Soft%20Target%20\(GST\)%20Specification.pdf](http://www.abd.uk.com/upload/files/2017-05-25_14-28-50_SP-6011%20Guided%20Soft%20Target%20(GST)%20Specification.pdf)
- [14] "Soft Car 360 Rev E." AB Dynamics. Accessed 07 04, 2017. http://www.abd.uk.com/upload/files/2017-05-25_14-29-06_SP-02%20Soft%20Car%20360%20Specification.pdf
- [15] DRI Advanced Test Systems. n.d. Soft Car 360. Accessed 07 04, 2017. <http://www.dri-ats.com/soft-car-360/>
- [16] Euro NCAP "Safety Assist." EuroNCAP. Accessed 07 04, 2017. <https://cdn.euroncap.com/media/26996/euro-ncap-aeb-c2c-test-protocol-v20.pdf>
- [17] "Safety Assist." EuroNCAP. Accessed 07 03, 2017. <https://cdn.euroncap.com/media/17719/euro-ncap-aeb-test-protocol-v11.pdf>
- [18] Moshon Data. n.d. Automotive Engineering. Accessed 07 04, 2017. <http://moshondata.com/products/engineering/>
- [19] Tecpond. n.d. UFO - ADAS Testing Tool. Accessed 07 05, 2017. <http://www.tecpond.at/ufo-adas-testing/>
- [20] I. Petterson, K. Johansson. "Characterization of visual and IR reflectivity of soft car targets". Luleå Technical University. 2018-06-25
- [21] S. Nord, M. Lindgren. "HiFi Visual Target - Methods for Measuring Optical and Geometrical Characteristics of Soft Car Targets for ADAS and AD". Lecture Notes in Mobility: Smart Systems Transforming the Automobile / [ed] Gereon Meyer, Berlin: Springer, 2017, pp. 201-209.

Appendix A – Portable Optical Instrument

As a part of the “HiFi Visual Target” project a portable optical reflectance measurement setup was developed. The setup is equipped to handle outdoor use in any weather conditions. All the parts are mounted inside an aluminium box with a lid.



The figure below shows how the parts of the portable measurement setup are connected. The iPad controls the laptop through TeamViewer. The laptop runs the software OceanView which controls the spectrometer and collects the measurements. The laptop is connected to the spectrometer through a USB cable. From the light source there are seven fibres that go to the measurement probe, six of the fibres transmits light from the light source and one of those fibres goes back to the spectrometer with the reflection.



A1 Spectrometer

The spectrometer used in the setup is an Oceanoptics OCEAN-FX-UV-VIS-ES spectrometer. This spectrometer can measure wavelengths from 200-1100 nm which was suitable for the measurements of visible light.



A2 Light source

The light source used in the setup is an HL-2000-LL which is a long-life tungsten halogen light source. This light source projects light with wavelengths from 360-2400 nm and lasts a minimum of 10,000 hours.



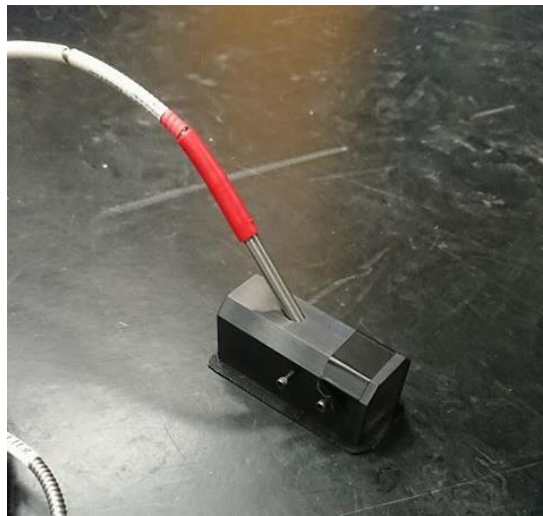
A3 Reflection Probe

The reflection probe used in the setup is an QR400-7-VIS-NIR which is capable of measuring light with wavelengths of 400-2100 nm. These fibres are protected with a stainless-steel sleeve which makes it suitable for outdoor use. The probe has a diameter of 6.35 mm. The fibre bundle has six illumination fibres surrounding one read fibre.



A4 Probe holder

To make sure all measurements are done the same way a probe holder is used. The probe holder is called RPH-1 and can be used for measurements with 45° angle as well as 90° angle.



A5 Integrating sphere

An integrating sphere is also used in the setup in place of the reflection probe. The sphere's model is ISP-50-8-R and has a spectral range of 200-2500 nm.



A6 Fibre cables

The fibre cables used in the setup are one cable QP1000-5-VIS-BX with a diameter of 1000 μm and one cable QP400-5-VIS-BX with a diameter of 400 μm .

A7 Battery pack

To power the spectrometer and the light source a battery pack is used. This battery pack has a capacity of 26000 mAh and can power the setup for a whole day without needing to recharge. There is also a second hot-swappable battery pack available.

A8 Software

The software used to acquire the measurements is Oceanview by Ocean Optics. To be able to use the setup in all weather conditions, an iPad with a waterproof cover is used to control a laptop with Oceanview installed. To do this, TeamViewer is used.